Traffic Flow Implications of Driverless Trucks

Microscopic traffic simulations using SUMO

William Erlandson

Department of Technology and Society

Lund University

29th April 2020

LTH, Institutionen för Teknik och samhälle CODEN: LUTVDG/(TVTT-5319)/1-94/2020 ISSN 1653-1922

Tryckt i Sverige av Media-Tryck, Lunds universitet Lund 2020

Examensarbete CODEN: LUTVDG/(TVTT-5319)/1-94/2020

Thesis / Lunds Tekniska Högskola,
Instutionen för Teknik och samhälle,
Trafik och väg, 352 ISSN 1653-1922

Author: William Erlandson

Title: Trafikflödeseffekter av Självkörande Lastbilar - Trafiksimulering i SUMO
English title: Traffic Flow Implications of Driverless Trucks - Traffic Simulations using SUMO
Language: English
Year: 2020
Keywords: Traffic Simulation; Driverless; Autonomous; AT; SUMO; Freight
Citation: William Erlandson. Lund, Lunds universitet, LTH, Institutionen för Teknik och samhälle. Trafik och väg 2020. Thesis 352

Abstract: The truck sector is thought to be one of the first adopters of autonomous driving technology. Reduced fuel- and labour costs, increased flexibility in scheduling and increased hours of service, are all incentives for the freight companies to go autonomous. The automation of the truck fleet is likely to be gradual. At first, autonomous trucks (AT:s) are expected to have a conservative driving style, avoid lane-changes and keep large gaps to the surrounding traffic. As technology advances, the AT:s will eventually be capable of performing any type of driving maneuvers and to a certain extent make use of vehicle-to-vehicle communication systems (V2V). In this thesis, the microscopic traffic simulation software SUMO is used to investigate how AT:s with a conservative driving style, and AT:s with enhanced driving capabilities, affect travel times, maximum road capacity and emissions of carbon dioxide. When simulating AT:s in a heterogeneous traffic flow, the conservative driving style turned out to have a negative effect on both maximum road capacity and average travel times. Congestion around an on-ramp that worked as a bottleneck, significantly increased when conservative AT:s were introduced. Total emissions of carbon dioxide, however, decreased. The AT with enhanced driving capabilities, showed a much better performance, with insignificant effects on travel times, increases in road capacity and decreases in emissions of carbon dioxide. It is therefore likely that, in early stages of AT deployment, the overall effect on traffic could be negative. Once the share of AT:s with enhanced driving capabilities increase, the effect is instead assumed to be positive.

The introduction of AT:s advocates an increased share of trucks at night, when there is free capacity available. In order to save energy, these AT:s would drive at much lower speeds than the surrounding traffic. Simulations show that nighttime AT traffic has limited effects on travel times but results in large increases in total emissions of carbon dioxide. The simulations showed that a very low traffic flow is crucial in order to ensure low emission levels. Introduction of nighttime AT traffic should therefore come with sufficient time- and route restrictions, in order to ensure ecological sustainability.

Trafik och väg
Institutionen för Teknik och samhälle
Lunds Tekniska Högskola, LTH
Lunds Universitet
Box 118, 221 00 LUND

Transport and Roads
Department of Technology and Society
Faculty of Engineering, LTH
Lund University
Box 118, SE-221 00 Lund, Sweden

Abstract

The truck sector is thought to be one of the first adopters of autonomous driving technology. Reduced fuel- and labour costs, increased flexibility in scheduling and increased hours of service, are all incentives for the freight companies to go autonomous. The automation of the truck fleet is likely to be gradual. At first, autonomous trucks (AT:s) are expected to have a conservative driving style, avoid lane-changes and keep large gaps to the surrounding traffic. As technology advances, the AT:s will eventually be capable of performing any type of driving manoeuvres and to a certain extent make use of vehicle-to-vehicle communication systems (V2V).

In this thesis, the microscopic traffic simulation software SUMO is used to investigate how AT:s with a conservative driving style, and AT:s with enhanced driving capabilities, affect travel times, maximum road capacity and emissions of CO_2. When simulating AT:s in a heterogeneous traffic flow, the conservative driving style turned out to have a negative effect on both maximum road capacity and average travel times. Congestion around an on-ramp that worked as a bottleneck, significantly increased when conservative AT:s were introduced. Total emissions of CO_2 however, decreased. The AT with enhanced driving capabilities, showed a much better performance, with insignificant effects on travel times, increases in road capacity and decreases in emissions of CO_2. It is therefore likely that, in early stages of AT deployment, the overall effect on traffic could be negative. Once the share of AT:s with enhanced driving capabilities increase, the effect is instead assumed to be positive.

The introduction of AT:s advocates an increased share of trucks at night, when there is free capacity available. In order to save energy, these AT:s would drive at much lower speeds than the surrounding traffic. Simulations show that nighttime AT traffic has limited effects on travel times but results in large increases in total emissions of CO_2. The simulations showed that a very low traffic flow is crucial in order to ensure low emission levels. Introduction of nighttime AT traffic should therefore come with sufficient time- and route restrictions, in order to ensure ecological sustainability.

Acknowledge

Firstly, I would like to pay my special regards to my supervisor at ITRL, Albin Engholm, for invaluable support throughout the entire thesis project. Thank you for insisting on using an open-source software for traffic simulations. It greatly improved my understanding for microscopic traffic modelling as well as my knowledge in Python programming.

I also wish to acknowledge the support from Louise Olsson at the Swedish Transport Administration. Thank you for assisting me from start to finish.

Furthermore, data provided by the Swedish Transport Administration as well as interviews with representatives from the vehicle manufacturers Einride and Scania, are truly appreciated. Without their support, the realisation of this thesis would not have been possible.

Lastly, I would like to show my gratitude to Dr. Rob Van Nes at TU Delft, for attracting my interest in traffic modelling. You clarified a complex subject in the most pedagogical way, laying the foundation of my subsequent studies.

William Erlandson, Stockholm 2020-04-29

List of Figures

List of Tables

Nomenclature

τ	Reaction time in seconds.
a	A vehicle's acceleration ability.
ABX	The minimum following distance in the Weidemann model.
AT	Autonomous truck
b	A vehicle's deceleration ability.
$Distance\ gap$	Distance in meters between a the rear of a vehicle and the front of its follower
$OPDV$	The point when a driver realises that the distance to the preceding vehicle is increasing in the Weidemann model.
SDV	The point when a driver realises that it is approaching another vehicle in the Weidemann model.
SDX	The maximum following distance in the Weidemann model.
T	Time headway in seconds between the rear of a leading vehicle and the rear of a following vehicle.
TC	Travel cost
TT	Travel time
TTC	Total travel cost
VoT	Value of time. A driver's valuation of a travel time reduction of 1 hour.
MPR_{AT}	Share of automation within the truck fleet.

Car-following parameters in SUMO

δ	Acceleration exponent in the IDM car-following model.
$sigma$	Parameter regulating driver imperfection.
tau	A vehicle's desired time headway T.

Vehicle type parameters in SUMO

speedDev	A vehicle's deviation from its desired speed.
speedFactor	A vehicle's desired speed in comparison to the speed limit.

Contents

1 Introduction

The development of automated driving technology is moving fast and will, when introduced in a large scale, have effects on traffic flow (Maurer et al., 2016). While this is certain, it is not yet known how. (Calvert, Schakel and Lint, 2017) state in their research article, that regardless of the outcome of research on this topic, the results will help mitigating future infrastructure costs. If vehicle automation was to negatively affect road capacities, infrastructure needs to be adapted in order to ensure stable traffic flows. Contrarily, if vehicle automation implies a substantial increase of capacity, the road infrastructure developments cannot continue like today.

According to (KPMG, 2019), the trucking industry is thought to be one of the first users of autonomous driving technology. Ginsburg and Uygur (2017) concur and states that a reason for this could be the plausible economic savings, the trucking industry could make by e.g. reducing fuel costs and enabling a more flexible route planning. Despite the expected future of autonomous freight transport, previous research on autonomous vehicles' effects on traffic has predominantly been focused on passenger vehicles (Kristoffersson and Brenden, 2018). This has resulted in a research gap that needs to be filled in order prepare for future freight traffic automation.

1.1 Previous work

The importance of investigating how self-driving vehicles affect traffic, is increasing due to the growing utilisation of driver-assistance systems (Kesting et al., 2008). Calvert, Schakel and Lint (2017) stated that we are currently in the beginning of a new era, where the driver of a vehicle is gradually replaced by computer based systems. Many researchers have studied how autonomous vehicles could potentially affect traffic flow in different future scenarios. Less attention has however, been given to the effects of automation within the freight sector. Ramezani et al. (2018) state that in the published research related to effects of autonomous trucks, there are yet fewer that use microscopic traffic simulations.

Ginsburg and Uygur (2017) discussed several ways that automation within the freight sector could affect traffic. First, implications of truck platooning was investigated. A platoon consists of several after another following trucks, that operate with small time headways. Theoretically, the result is increased capacity as more vehicles can pass a cross-section of a road at a particular time interval. The authors mentioned, however, that long platoons of trucks could generate driving difficulties for the surrounding traffic, which in turn would affect the traffic flow negatively (Ginsburg and Uygur, 2017). Despite this, the capacity effect was assumed to be generally positive. Autonomous trucks will drive with less speed fluctuations compared to manually driven vehicles, which reduces the risk of congestion. The authors further mentioned that AT:s without vehicle-to-vehicle communication systems are thought to make the

total road capacity increase linearly with an increasing number of AT:s, whereas AT:s equipped with vehicle-to-vehicle communication systems would result in a faster capacity increase. (Ginsburg and Uygur, 2017).

Müller (2012) used a microscopic simulation approach to investigate traffic implications of AT platoons. A 5 kilometer long network with two to three lanes and without intersections was used. In a platoon, vehicles are following the behaviours of a leader, which is the very first vehicle in the vehicle string. If it starts to break, the following vehicles react simultaneously, making the platoon act like a single vehicle unit. Müller (2012) captured this behaviour by modelling each platoon as a long single vehicle that used manual driving characteristics. The results showed that when 25 % of the vehicles were platooning, the capacity increased with approximately 5 %.

Ramezani et al. (2018) used a refined version of the CACC car-following model, developed by Milanés and Shladover (2014), in order to simulate implications of truck platoons, on Interstate 710 in Long Beach, California (Information about car-following models can be found in chapter 2.3). The network was approximately 24 kilomteres long and had 3 to 6 lanes. All automated trucks were assumed to be equipped with vehicle-to-vehicle communication systems (V2V), enabling them to communicate with other trucks and form platoons. In contrast to the simulations by Müller (2012), the trucks equipped with CACC technology could form platoons during the ongoing simulation and did thus not need to be predefined. The results showed a positive effect on both traffic flow and average speed. Müller (2012) however, discussed the works of Henning, Preuschoff and Happe (2003), where different results were obtained when simulating CACC-equipped trucks. The simulations showed that the increase in capacity that platooning could potentially generate, was compensated by disturbances caused by the coupling procedure of the platoon.

Calvert, Schakel and Lint (2017) discussed the future of trucks with V2V communication systems. They argued that when simulating a future scenario with heterogeneous flows of regular and autonomous vehicles, one should to a certain extent try to avoid relying on V2V communication systems. The penetration rate of the system is likely to be much lower than the total share of autonomous trucks, which results in a traffic flow with a variety of vehicle technologies.

Kristoffersson and Brenden (2018) investigated different scenarios of future freight automation by hosting a panel discussion with people working in the freight sector. The panel mentioned increased night driving as a possible effect of automation within the freight sector. This because drivers' working schedules would no longer need to be considered when planning the transport routes. Analogously, removing the driver would also enable the trucks to drive at lower speeds to save energy.

Energy saving and CO_2 emissions are recurring subjects within the research on autonomous freight transport. Ginsburg and Uygur (2017) stated that AT:s have the potential to cut fuel consumption and emissions within the freight sector since they will drive with less speed fluctuations compared to regular trucks. Sugimachi et al. (2013) on the other hand mentioned the decreased inter-vehicular spacing as a reason for a more energy- and fuel efficient freight transport, when using autonomous vehicles. A smaller gap to the preceding vehicle entails less air resistance which in turn reduces the energy

consumption (Sugimachi et al., 2013). This effect is even greater when the trucks drive in a platoon, where inter-vehicular distances are kept at a minimum.

As cited researchers have shown, there are several studies that have investigated the behaviour and effects of autonomous trucks, in a variety of transport networks. Many of which, did however, focus on the effects of platooning and advanced V2V communication systems. It is likely however, that within a foreseeable future, lower levels of automation will be introduced first (Calvert, Schakel and Lint, 2017). Later in development, the traffic flow is likely to consist of vehicles with a variety of automation technologies. This thesis therefore aims at investigating how autonomous trucks without V2V communication systems could affect traffic flow. Two types of autonomous trucks are defined, one with a conservative driving style, which represent AT:s in an early stage of development and one with an aggressive driving style, representing a further developed AT. This will capture how the AT:s' driver behaviour affects different aspects of traffic flow, such as maximum capacity, travel times and CO_2 emissions.

Furthermore this work will investigate the traffic flow implications of a distribution of AT:s, with and without V2V communication systems. Current research, such as Ramezani et al. (2018), has covered the positive traffic flow effects of trucks equipped with V2V communication systems. However, microscopic simulations with such AT:s in a heterogeneous flow of other types of AT:s with lower levels of automation, is currently missing. This work aims at filling this research gap.

Lastly, this thesis will analyse how total emissions of CO_2 change when introducing the above mentioned AT types. Research shows that autonomous vehicles, including AT:s, have the potential to decrease CO_2 emissions and energy consumption (Kristoffersson and Brenden, 2018). However, how emissions from the entire traffic flow change, including regular cars and trucks, has until not been investigated. By measuring the total amounts of emitted CO_2 during each simulation, this work tries to answer this question.

1.2 Purpose statement

The purpose of this thesis is to investigate how autonomous trucks (AT:s) could affect traffic flow, once they are introduced in a large scale. Three scenarios are created which represent different aspects of autonomous freight transport in an urban motorway setting. The scenarios are simulated in a microscopic traffic simulation software, in order to study how autonomous trucks affect travel times, travel costs, maximum road capacity and emissions of CO_2.

1.3 Research questions

The thesis will aim at answering the following research questions:

- How do AT:s without V2V communication systems affect travel times, travel

costs, total emissions of CO_2 and maximum road capacity, when introduced in an urban motorway setting?

- How does a distribution of AT:s with and without V2V communication systems affect travel times, travel costs, total emissions of CO_2 and maximum road capacity, when introduced in an urban motorway setting?
- How does slow AT traffic at night affect travel times and emissions of CO_2?

1.4 Geographical setting

In this thesis a road network consisting of an 8.6 kilometre long motorway section with two grade-separated intersections. In order to make the infrastructure and the traffic as realistic as possible, the network was modelled to replicate a section of a real existing motorway. When looking for a suitable geographical location, there were several aspects to bear in mind. Firstly, the motorway should be located in an environment where the traffic flow is high and sometimes reaches capacity. This would facilitate the analysis of the autonomous trucks' effect on total road capacity. Secondly, the motorway section should contain a number of on- and off-ramps with considerable traffic, which would act as bottlenecks in the network. Lastly there should be sufficient data on e.g traffic volumes, vehicle distributions and time headways in order to replicate the transport system well.

A section of motorway E6 in central Gothenburg, Sweden, turned out to fulfill all the above mentioned criteria. E6 is one of Scandinavia's most important highways, connecting Trelleborg in the southernmost part of Sweden with the Norwegian town Kirkenes above the arctic circle (*E6 Highway Project* 2020). Through central Gothenburg, on the west coast of Sweden, E6 has three lanes in both the northbound and southbound direction and has grade-separated intersections. The speed limit is restricted to 70 km/h through the urban area, which differs from the standard speed limit of 110 km/h on rural parts of the motorway (NTF, n.d.). At Gårda intersection (see figure 1.1), there are loop detectors which collect information on vehicle flows, speeds and vehicle distributions. Data from the detectors was provided by Trafikverket (2019). More information about the road network in the simulation model is shown in chapter 3.3. A picture showing the topology of the network model is shown in figure 3.3.

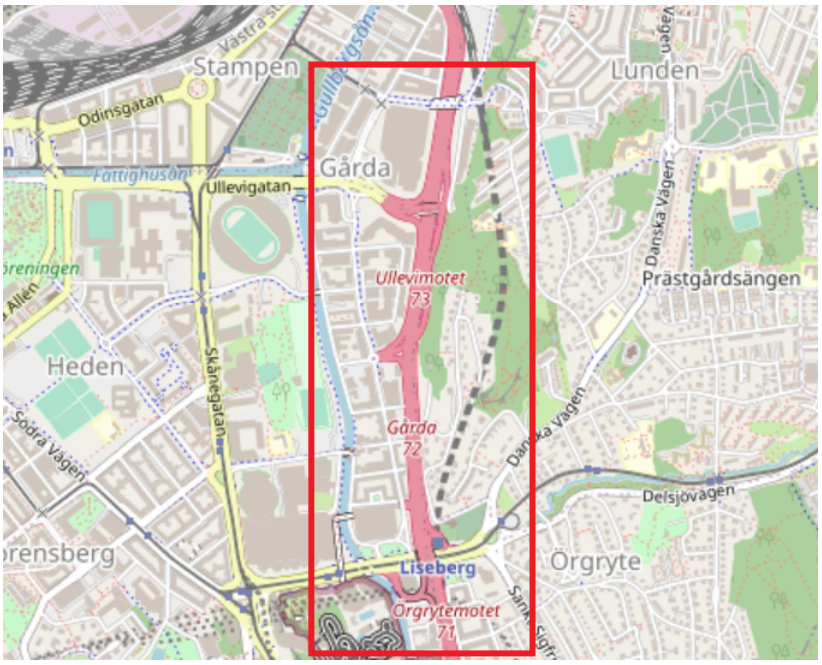

Figure 1.1: Location of the motorway network modelled in this thesis. The road section in pink represents motorway E6 in central Gothenburg. Source: *OpenStreetMap* (2020).

1.5 Scope and limitations

As mentioned above, the purpose of this study is to explore traffic flow effects of autonomous trucks in an urban motorway setting. The focus is therefore on infrastructure with grade-separated junctions and median dividers, which prevents the traffic flow in one direction from interacting with the flow in the opposite direction. The simulated vehicles are thus not exposed to a range of traffic situations that normally occur during an average trip, such as over-takings in the opposite direction lane, giving way to vehicles approaching from the right in intersections, driving trough signalled intersections as well as interacting with pedestrians and cyclists. Consequently, there are several aspects of traffic with autonomous trucks that this work will not cover.

The geographical setting entails further limitations to this work. The speed limit on the investigated part of motorway E6 in Gothenburg is 70 km/h, which differs significantly from rural sections of the Swedish motorway network, where the standard speed limit is 110 km/h (NTF, n.d.). As a consequence, the results presented in this work cannot be used to draw conclusions about AT vehicles' general effects on traffic flow under circumstances that differ significantly from those modelled in this thesis.

A vehicle's travel time, average speed and emission of CO_2 relate to the stability of the traffic flow. If the flow starts to break down, and starts showing a stop-and-go behaviour, the average speed is reduced, which increases the travel time. The probability of flow breakdown correlates with the occurrence of bottlenecks, such as on-ramps or merging lanes in the network. In the network simulated in this thesis, the geographical spread is limited and only covers two on-ramps. As a result, flow

characteristics shown in the simulations might differ significantly from the real traffic flows on motorway E6 through Gothenburg. Congestion at a particular cross-section could appear before the flow rate reaches capacity, due to traffic breaking down further ahead in the network. The aim of the thesis is thus not to relate the results to the infrastructure at the particular location in Gothenburg, but instead, in a more general sense, to study AT vehicles' effects on traffic flow, given the circumstances defined in the model.

Lastly, when simulating vehicle emissions in this work, it is assumed that all vehicles, including the AT:s, run on fossil fuels. No data on the characteristics of vehicles on the route has been considered. A share of today's vehicles use other fuels than gasoline and diesel, which means that the emission results shown in this thesis might be slightly exaggerated.

1.6 Thesis structure

The thesis is structured as follows. Chapter 2 contains a literature review, in which the most relevant aspects of autonomous vehicles and microscopic traffic modelling is presented. Chapter 3 describes the methodology used throughout this thesis, including the model structure, model calibration and simulated scenarios. Chapter 4 presents the results from each simulation and in chapter 5, the results are discussed an analysed. Lastly, in chapter 6, conclusions are drawn, based on the presented results.

2 Literature review

2.1 Autonomous vehicles

The autonomous vehicle technology is developing fast and is to be commercially available during the coming decade, according to Gordon et al. (2018). The autonomous vehicle technology is divided into 6 levels by the Society of Automobile Engineers (SAE, 2019). It ranges from 0 (no autonomous technology) to 6 (full automation, no actions from driver is needed). The lower levels of automation contain e.g. break- and acceleration control, lane-keeping assistance and adaptive cruise control (SAE, 2019). Some technologies are currently available in modern passenger cars, whereas technologies in the higher levels of automation are still to be developed. Tettamanti, Varga and Szalay (2016) argue that in the initial phase of vehicle automation development, the driver behaviour will be conservative, with large time headways to surrounding traffic and as a result, there will be a loss of road capacity. Later on in development, however, the authors predict an opposite effect. They further argue that the driver behaviour of an automated vehicle will be more deterministic than that of a regular vehicle and have significantly lower reaction times (Tettamanti, Varga and Szalay, 2016).

2.1.1 Adaptive Cruise Control (ACC)

The Adaptive Cruise Control system is based on the regular cruise control systems (CC), that makes a vehicle keep a particular speed that is determined by the driver (Kesting et al., 2008). If there are no preceding cars ahead in the same lane, the vehicle equipped with the CC system can keep this desired speed. However, if the flow of cars increases, and there are slower vehicles ahead in the same lane, the driver needs to deactivate the CC system, by manually breaking the vehicle. A vehicle equipped with Adaptive Cruise Control technology, on the other hand, automatically adjusts its speed according to the speed difference and distance to the preceding vehicle (Kesting et al., 2008). Figure 2.1 shows an ACC-equipped vehicle following another vehicle. Radar is used to calculate the distance gap x_r and the relative velocity to the vehicle in front v_r, from which the preferred velocity v_h and acceleration a_h is determined (Naus et al., 2010).

Several traffic simulations have indicated that ACC-equipped vehicles could have a positive effect on road capacity. Kesting et al. (2008) simulated an increasing market penetration rate of ACC-equipped cars on a 13 km long 3-lane motorway with an on-ramp that generated significant congestion problems. The simulations showed that already at a market penetration rate of 25 %, the congestion was eliminated. Despite this, the ACC technology has its deficits. Milanés and Shladover (2014) showed through experiments that when many ACC-equipped vehicles drove in a platoon, the ACC-system did not prove string stability. When the very first vehicle in the platoon started breaking, the following vehicle reacted by breaking harder than the first

vehicle. This resulted in an amplification of the breaking reactions backwards in the platoon, making the last vehicle decelerate much more than the first vehicle (Milanés and Shladover, 2014). The authors therefore stated that an increased market penetration rate could make the traffic flow less stable. According to the authors, the reason the simulations have not indicated the string stability issues shown in the experiments, is that the they have underestimated the time the ACC needs to react to changes to the preceding vehicle's speed (Milanés and Shladover, 2014).

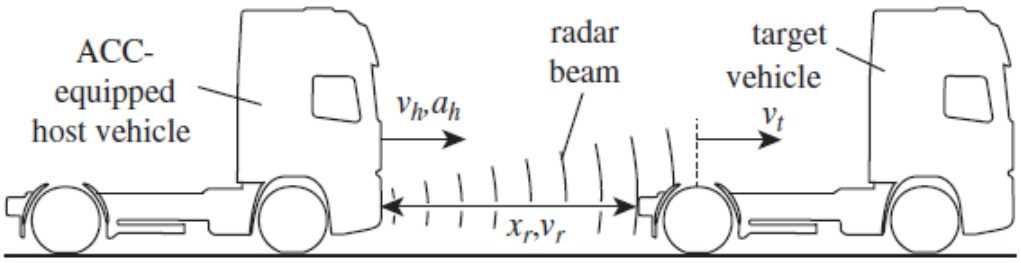

Figure 2.1: Structure of the ACC system. Source: Naus et al. (2010)

2.1.2 Cooperative Adaptive Cruise Control (CACC)

The Cooperative Adaptive Cruise Control (CACC) make use of the speed control systems found in ACC techonologies, but extends it by implementing Vehicle-to-Vehicle (V2V) communication systems (H. Liu et al., 2018). The V2V communication enables vehicles to drive with much smaller time gaps than regular vehicles, since they can communicate with vehicles further ahead in the same lane, and thus react to speed changes earlier. H. Liu et al. (2018) state that a CACC-equipped vehicle can use a time gap of only 0.6 seconds, compared to the average time headway on motorways, which is 1.4 seconds. Milanés and Shladover (2014) further showed that, unlike the ACC system, the CACC system was string stable when implemented on a platoon of cars. In contrast to an ACC-equipped vehicle, a vehicle with CACC technology can react to speed changes made by any vehicle in the platoon, which drastically reduces the reaction time and improves the string stability (Milanés and Shladover, 2014).

2.2 Traffic modelling

Traffic models are used to experimentally analyse traffic flow characteristics in a transport system (Linköping University, 2020). The models use mathematical formulas in order to replicate e.g vehicles' driving behaviours or traffic densities on a particular road section. Traffic models have been used for a long time - the first models that were based on traffic flow theories were developed by Bruce D. Greenshield already in the 1930's (Treiber and Kesting, 2013). Due to increased traffic flows in urban areas and development within computer science, traffic models have become very useful tools in transportation planning in recent years.

There are several types of traffic models and they can be categorised in various ways (Treiber and Kesting, 2013). One common way to differentiate them is by the level of network aggregation. In a macroscopic traffic model, traffic is modelled as aggregated flows in an extensive road network with little detail (see figure 2.2). In a microscopic model on the other hand, the network contains higher level of detail and every single vehicle is modelled as a separate unit. Mesoscopic traffic models use a level of detail that is in between the macroscopic and the microscopic models. (see figure 2.2). In sections 2.2.1 and 2.2.2 below, macroscopic and microscopic traffic models are described.

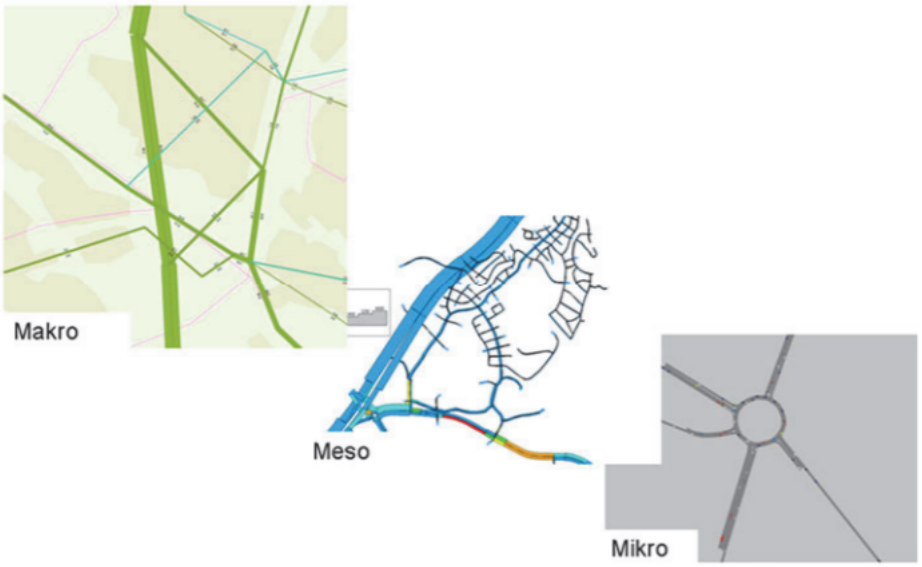

Figure 2.2: Categorisation of traffic models based on the representation of reality. Source: Trafikverket (2013).

2.2.1 Macroscopic traffic modelling

A typical case when macroscopic traffic modelling is used is when making traffic forecasts (Trafikverket, 2014). The forecast modelling has four distinctive steps:

1 Traffic generation

2 Destination choice

3 Mode choice

4 Traffic assignment

In the first step the observed area or region is divided into a number of zones, each with different spatial characteristics. Based on data on a range of parameters, such as population, income, car-ownership etc. the number of journeys generated within the zone (the transport demand) and the number of journeys attracted by the zone are calculated. Secondly the transportation demand between all zones are calculated

which results in an origin-destination-matrix. In step 3 the traffic between all zones are divided between each available transport mode, e.g car, bus, train etc. Lastly the traffic is assigned to routes through the network, which generates flows on each link. The output from step 4 affects both the mode- and destination choice - if a link gets congested people would pick an alternative route to get to their destination. As a result, step 2, 3 and 4 are calculated again and continues to do so iteratively until an equilibrium is found (Trafikverket, 2014).

In a macroscopic traffic model (traffic assignment), the flow of vehicles in a road network is modelled similar to fluids (Treiber and Kesting, 2013). Formulas describing the conservation of mass are thus also applicable for a transport system. If one considers a section of a road, the number of vehicles entering from one side must equal the number leaving it at the other end, given the absence of on- and off ramps along the road section. The conservation of vehicles is given by equation 2.1, where δ_k is the change in traffic density during time step δ_t and δ_q is the change in traffic flow along the road section δ_x (L. V. Knoop, 2017). This could also be written as a partial differential equation as shown in equation 2.2.

$$\frac{\delta_k}{\delta_t} + \frac{\delta_q}{\delta_x} = 0 \tag{2.1}$$

$$\partial_t \cdot k + \partial_x \cdot q = 0 \tag{2.2}$$

Another important formula in macroscopic traffic modelling relates to the relation between traffic density k, speed u and flow rate q (see equation 2.3). This equation forms fundamental diagrams that can be shown graphically (see figure 2.3). With the flow q defined as a function of the density k, equation 2.2 can be rewritten according to equation 2.4. This forms the definition of the Lighthill-Whitham-Richards (LWR) model which is based on the conservation of vehicles and a fundamental diagram (L. V. Knoop, 2017).

$$q = ku \tag{2.3}$$

$$\partial_t \cdot k + \partial_x \cdot f(k) = 0 \tag{2.4}$$

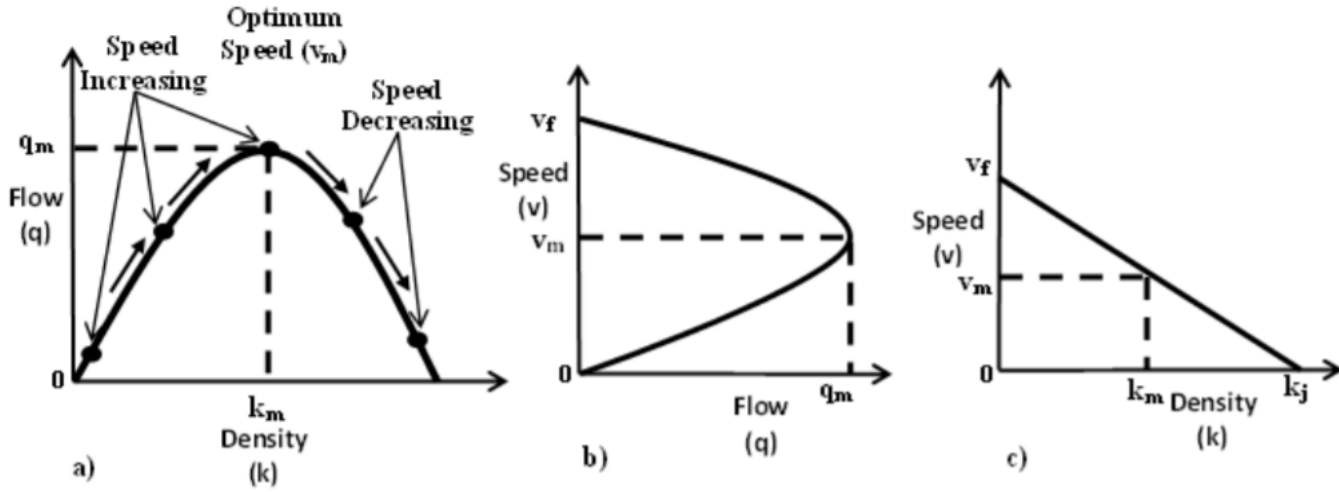

Figure 2.3: Fundamental diagrams in traffic flow theory. Source: Zaidi et al. (2015).

2.2.2 Microscopic traffic modelling

In microscopic traffic modelling, traffic is modelled as a stream of discrete vehicles (Treiber and Kesting, 2013). Time is the independent variable and every simulated vehicle's longitudinal and lateral position, speed and acceleration are calculated during every time step of the simulation (Tapani, 2008). Figure 2.4 shows how a microscopic model represents reality. During a small time step dt the change in speed dv for vehicle α is a function of e.g the acceleration α, the current speed v, distance gap to a leading vehicle s and difference in speed between vehicle α and a leading vehicle in the same lane.

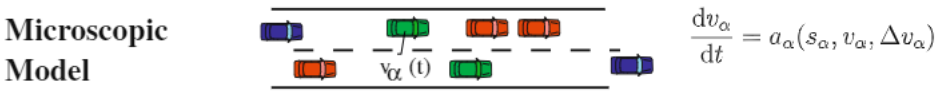

Figure 2.4: Description of how a microscopic traffic model represents reality. Source: Treiber and Kesting (2013).

When simulating the longitudinal vehicle movements on any type of infrastructure, each vehicle's speed and acceleration will be affected by the behaviours of the surrounding traffic. If a leading vehicle has a lower speed than the following vehicle in the same lane, the following vehicle might have to decelerate in order to maintain its desired safety time headway, T, to the leading vehicle. Correspondingly, if the leading vehicle then accelerates, the following vehicle will react by increasing the speed to its desired speed. In microscopic traffic simulations such vehicle movements are managed by a car-following model (Krauß, 1998). It controls only the longitudinal vehicle movements and does thus not allow the vehicle to pass the leading vehicle. Lateral movements, such as lane changing on motorways and overtakings on two-lane roads, are controlled by separate lane-changing models and overtaking models (Olstam J., 2004). Car-following models are treated in chapter 2.3 whereas information about

lane-changing models is found in chapter 2.5.

2.3 Car-following models

A car-following model controls a vehicle's longitudinal movements, such as acceleration and deceleration in response to the driving behaviour of a leading vehicle in the same lane. According to Krauß (1998), there is a fundamental function that most common car following models are based on (see function 2.1). It says that the momentary acceleration of a vehicle i, at a timestep t, is a function of the difference between the desired velocity V_{des} and the current velocity v_i and some "sensitivity" parameter τ. The desired speed V_{des}, usually is a function of the speed of the preceding vehicle, $v_{t+1}(t)$. (Krauß, 1998).

$$\frac{dv_i(t)}{dt} = \frac{V_{des}(t) - v_i(t)}{\tau} = f(v_{i+1}(t), v_i(t), \tau) \tag{2.5}$$

In continuous car-following models, time is considered as a continuous variable which means that a following vehicle's acceleration is calculated at any point in time. This results in several differential equations that describe the behaviour of a vehicle following another (Treiber and Kesting, 2013). In discrete car-following models, time is not continuous, but instead a range of discrete values. In every time step, the acceleration of the following vehicle is calculated as a function of the results in the previous time step. Discrete car-following models cannot replicate real traffic situations as well as continuous models, but due to their simplicity, they need less computing power and could thus still be advantageous (Treiber and Kesting, 2013). In the following sections, the most commonly used car-following models are described briefly.

2.3.1 The Krauss model

The Krauss car-following model is the default car-following model, used in the traffic simulation software SUMO (German Aerospace Center, 2019d). It was developed by Stefan Krauß at the German Aerospace Center in 1998 (Krauß, 1998). It is categorised as a "Safe Distance Model", since it is based upon the assumption that a driver will adjust its speed in such a way that a desired distance to the preceding vehicle is kept at all times (Kanagaraj et al., 2013).

A following vehicle's speed is determined by first calculating a maximum safe speed, v_{safe}. It is defined as the highest speed a vehicle can keep, without colliding with the preceding vehicle in the same lane. v_{safe} is given by formula 2.6, where $v_l(t)$ is the current speed of the leading vehicle, $g(t)$ is the distance gap to the leading vehicle, τ is the reaction time, $\bar{v}(t)$ is the average speed of the leading and the following vehicle and b is the maximum deceleration ability (Jost and Nagel, 2005).

After the safe speed has been calculated, the vehicle's desired speed, v_{des}, can be calculated. v_{des} is the speed the vehicle would like to reach, given the v_{safe} constraints

defined in formula 2.6 below. v_{des} is given by formula 2.7, where $v(t)$ is the vehicle's current speed, $a\Delta t$ is the speed increase during the current time step and v_{max} is the vehicle's maximum speed. .

v_{des} enables the calculation of the vehicle's resulting speed in the next time step. This is given in formula 2.8 where ϵ is the noise amplitude, a is the maximum acceleration ability and η is a random number between 0 and 1 (Jost and Nagel, 2005). The term $\epsilon a \eta$ adds a random element to the desired velocity which captures the stochastic characteristics of a human driver. When the resulting speed has been determined for each vehicle in the simulation, the vehicles' positions are updated according to formula 2.9.

$$v_{safe}(t) = v_l(t) + \frac{g(t) - v_l(t)\tau}{\frac{\bar{v}(t)}{b} + \tau} \tag{2.6}$$

$$v_{des}(t) = min\{v(t) + a\Delta t, v_{safe}, v_{max}\} \tag{2.7}$$

$$v(t + \Delta t) = max\{0, v_{des} - \epsilon a \eta\} \tag{2.8}$$

$$x(t + \Delta t) = x(t) + v(t + \Delta t) \cdot \Delta t \tag{2.9}$$

2.3.2 Intelligent Driver Model (IDM)

The Intelligent Driver Model is a commonly used time-continuous car-following model that belongs to the Gazis-Herman-Rothary (GHR) group of models (Pourabdollah et al., 2018). In this group of models, the acceleration a of a vehicle i, is calculated as a function of the preceding vehicle's speed v_{i-1} and the distance gap to the preceding vehicle s_i.

In the IDM model, the acceleration of vehicle i at time t is given by formula 2.10, where a_{max} is the vehicle's maximum desired acceleration, $v_i(t)$ is the vehicles speed at timestep t, $v_{des}(t)$ is the vehicles desired speed at timestep t, δ is an acceleration exponent and s_i is the distance gap to the preceding vehicle i. The parameter s_i^* is given by formula 2.11.

The IDM model has historically been a common choice of car-following model when simulating autonomous vehicles (Calvert, Schakel and Lint, 2017). Modified versions of the IDM model has also been used in experimental autonomous vehicles. Milanés and Shladover (2014) found however, that when applied to a cars in their field experiments, the model generated significant delays in the response to speed changes.

$$a_i(t) = a_{max} \cdot (1 - \frac{v_i(t)}{v_{des}(t)})^{\delta} - (\frac{s_i^*}{s_i})^2 \tag{2.10}$$

$$s_i^* = s_0 + v_i(t) \cdot T + \frac{v_i(t) \cdot \Delta v_i(t)}{2 \cdot \sqrt{a_{max} \cdot b_{max}}} \tag{2.11}$$

2.3.3 Wiedemann model

The Wiedemann model is a psycho-social time continuous car-following model that is used by the traffic simulation software VISSIM (Treiber and Kesting, 2013). The model's psycho-social nature brings that a following vehicle reacts to speed changes of the preceding vehicle only if the speed change is larger than a particular threshold. Treiber and Kesting (2013) state that this captures the behaviour of human drivers in a better way than the models that react to infinitely small speed changes. Tettamanti, Varga and Szalay (2016) however, argue that psycho-social, as previously used, will not capture the behaviours of autonomous vehicles very well. The parameters used in psycho-social models are based on statistics on human driver behaviours. Since the driver behaviour of autonomous vehicles will be deterministic in comparison to human driven vehicles, the psycho-social models need to be adjusted to match this behaviour (Tettamanti, Varga and Szalay, 2016).

The Wiedemann model determines a vehicle's acceleration based on four regimes:

1 Free flow

2 Approacing a preceding vehicle

3 Car-following close to a steady-state equilibrium

4 Critical situations

In each regime, the acceleration is calculated differently. The regimes are shown in figure 2.5. The blue line symbolises a car approaching a slower vehicle in the same lane. Once the threshold for detecting the preceding vehicle is passed (SDV), the vehicle reacts by decelerating with an acceleration determined by regime 2, causing the speed difference between the vehicles, Δv, to decrease. Once Δv is sufficiently small, the car-following regime (regime 3) is activated, making the acceleration oscillate around $\Delta v = 0$. (Treiber and Kesting, 2013). The regimes in figure 2.5 are defined by functions in a three-dimensional space, $f(s, v, \Delta v)$, spanned by the gap to the preceding vehicle (s), the following vehicle's speed (v) and the speed difference Δv. The regime borders are thus in fact surfaces rather than curves as pictured in figure 2.5 (Treiber and Kesting, 2013).

2.3.4 ACC

The ACC car following model was developed by Milanés and Shladover (2014) to enable simulation of vehicles equipped with adjustable cruise control technologies. As mentioned in chapter 2.3.2, the IDM model had previously been commonly used when simulating autonomous vehicles. However, after using the IDM car-following

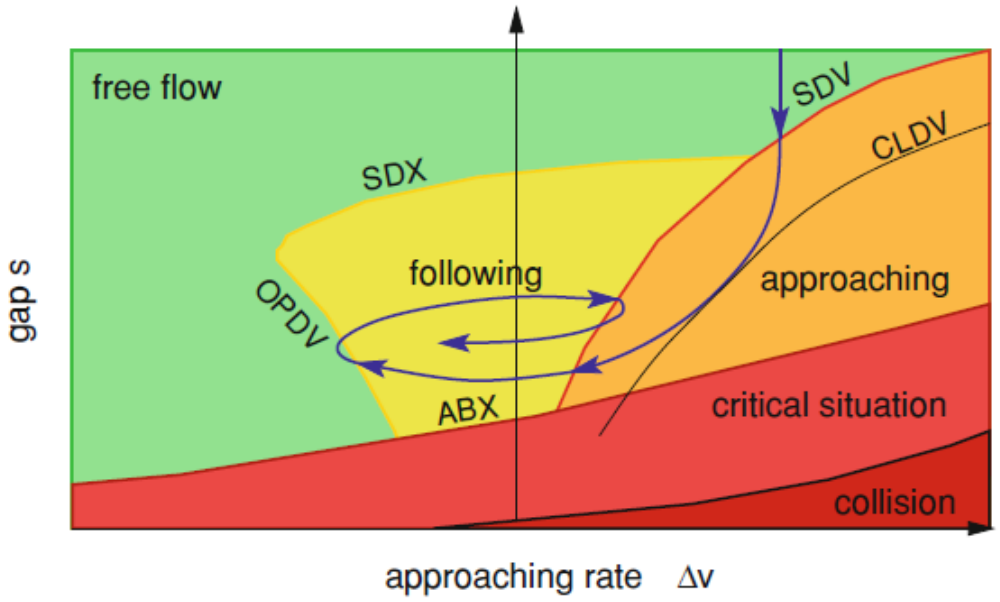

Figure 2.5: Regimes in the Wiedemann car-following model. Source: Treiber and Kesting (2013).

.

model on experimental vehicles, Milanés and Shladover (2014) questioned the IDM model's ability to react to a leading car's speed changes. They therefore came up with a car-following model specific for ACC vehicles, that turned out to generate a better car-following behaviour (Milanés and Shladover, 2014). In the ACC model, the acceleration of a vehicle k, is calculated with formula 2.12, where x_{k-1} is the position of the preceding vehicle, x_k is the position of the subject vehicle k, v_{k-1} is the speed of the preceding vehicle and v_k is the speed of the subject vehicle. t_{hv} is the desired time gap to the preceding vehicle and k_1 and k_2 are weights, determining the importance of the distance and the speed difference respectively. By minimising the error between the simulation results and the data from the experimental vehicles, $k_1 = 0.23\ s^{-2}$ and $k_2 = 0.07\ s^{-1}$ was found to generate the best fit (Milanés and Shladover, 2014).

$$a_k = k_1(x_{k-1} - x_k - t_{hv}v_k) + k_2(v_{k-1} - v_k) \tag{2.12}$$

Since the ACC model was created to replicate the behaviour of vehicles equipped with ACC technologies, and k_1 and k_2 was tuned in order to minimise the error between the simulation results and the results from the field experiments, the string instability that was shown in section 2.1.1 also applies for the ACC model (Milanés and Shladover, 2014). The authors mention that k_1 and k_2 could be adjusted to increase the string stability, but that could worsen other aspects of the car-following behaviour.

2.3.5 CACC

The CACC car-following model was developed by Milanés and Shladover (2014) in order to mimic the driving behaviour of autonomous vehicles equipped with V2V

communication systems. The simulated vehicles using the CACC-model can communicate to other surrounding vehicle, react to their speed changes and form platoons. In contrast to the ACC car-following model, described in section 2.1.1, the CACC model showed string stability when simulating a string of four cars (Milanés and Shladover, 2014). The CACC model uses the gap error e_k to determine the vehicle speed. The gap error is equal to the formula that is multiplied with k_1 in the ACC model (see formula 2.12). It is defined as the difference between the actual distance between the vehicles and the desired distance gap (see formula 2.13). If e_k is positive, i.e. the distance between the subject vehicle and the preceding vehicle is larger than desired, it causes the subject vehicle to accelerate (Milanés and Shladover, 2014).

The subject vehicle's speed is calculated from e_k and its derivative $\dot{e}_k$ (see formula 2.14). v_{kprev} is the initial vehicle speed and k_p and k_d are weights that determine the impact of e_k and $\dot{e}_k$ respectively, on the resulting speed, v_k. Milanés and Shladover (2014) used $k_p = 0.45$ and $k_d = 0.25$.

$$e_k = x_{k-1} - x_k - t_{hv} v_k \tag{2.13}$$

$$v_k = v_{kprev} + k_p e_k + k_d \dot{e}_k \tag{2.14}$$

2.4 Headway distributions

Even though networks in microscopic traffic simulations aim at being realistic and representing real-world traffic networks as well as possible, they contain simplifications that need to be considered when running simulations. In a real-world traffic network, the geographical spread is very large, which means that the vehicle flow at a particular cross-section is a result of the driving behaviours of numerous vehicles in the network. In a microscopic simulation however, the traffic flow inside the model is a result of predefined inflows. In order to generate realistic traffic heterogeneity, the traffic flow entering the simulated network needs to follow a stochastic distribution (Treiber and Kesting, 2013). The stochastic distribution used in this model is described in chapter 3.

Several research articles have investigated and compared stochastic distributions when explaining time headways, T, at different traffic flows. If one assumes that the time headway is represented by the stochastic variable X and the traffic flow per hour is denoted q , the average time headway can be calculated calculated as:

$$\lim_{x \to \infty} \frac{\sum_{i=1}^{n} X_n}{n} = \frac{1}{\frac{q}{3600}} = \frac{3600}{q} \tag{2.15}$$

The time headways do, however, not distribute themselves symmetrically around the average. As Figure A.1 shows, the time headway distribution on the Long Island Expressway in New York City was proven to be asymmetrical with a peak at around 2

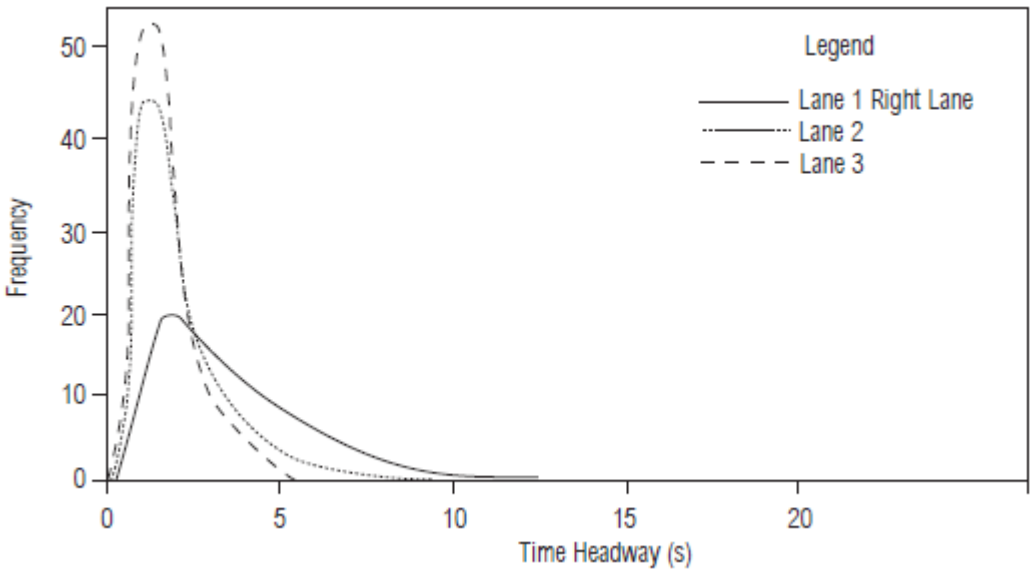

Figure 2.6: Time headway distributions on the Long Island Expressway in New York. Source: TRB, 2000

Table 2.1: Measured mean headways and standard deviations on motorway I-35 in Austin, Texas. Source: Ye and Zhang (2009)

Flow	< 800 veh/h		800-1500 veh/h		> 1500 veh/h	
Headway type	μ	σ	μ	σ	μ	σ
Car following Car	8.38	9.05	4.16	3.29	1.95	1.52
Truck following car	8.76	9.01	6.39	3.72	2.61	1.87
Car following truck	1.87	9.46	9.14	5.02	2.55	1.50
Truck following truck	9.12	9.56	9.42	6.08	2.75	1.54
Mixed	8.84	9.18	5.03	4.03	2.06	1.57

seconds (TRB, 2000). Time headways larger than the peak value was observed more frequently than smaller time headways. This could partly be explained by the fact that T has no upper limit but is downwards limited by a minimum safety headway. Figure 1 further shows that the dispersion of T in the adjacent lanes 2 and 3 is smaller and has a more uniform distribution (see figure A.1).

According to Greenberg (1966), the log-normal distribution was proven to generate a good fit to time headway data. By fitting a log-normal distribution to both data from a Californian freeway, as well as data from the Holland tunnel in New York City, he proved that the log-normal distribution was able to describe the headways in both data sets. Ye and Zhang (2009) instead used vehicle type specific headway data in order to fit a distribution to each vehicle combination. In table 1, the results from their analysis is shown. They found that the largest mean time headway occurs when a car follows a truck. Another finding was that the standard deviation in the data decreased for all vehicle combinations when the traffic flow increased. This means that the data is distributed more closely around the mean at high traffic flows.

2.5 Lane changing models

Apart from vehicles' longitudinal accelerations, the traffic flow is also affected by the lateral vehicle maneuvers such as lane changes (Moridpour, Rose and Sarvi, 2009). In order to perform lane changes, a vehicle needs to adjust its speed to the traffic in the adjacent lane. Sometimes, also the traffic in the adjacent lane needs to adjust its speed to give the lane-changing vehicle sufficient space. A result could be a capacity drop that can spread backwards in both lanes (Moridpour, Rose and Sarvi, 2009). In order to simulate traffic realistically, modelling vehicles' lateral movements is therefore of great importance.

In microscopic traffic simulations, lateral movements are determined by a separate *lane-changing model*. As of 2019, SUMO supports three different lane changing models: LC2013, SL2015 and DK2008 (German Aerospace Center, 2019a). The DK2008, created by Daniel Krajzewicz, was the model that was first used by the simulation software and was the default lane-changing model until the release of SUMO version 0.18.0. LC2013, is the current default lane-changing model, created by Jakob Erdmann as an expansion of the previous DK2008 model. The SL2015 model is used when increased lateral resolution is needed (German Aerospace Center, 2019a). Since LC2013 is the default lane changing model, it will be described in further detail below.

2.5.1 LC2013

The LC2013, developed by Erdmann (2015) considers a vehicle's planned route, in order to calculate the need for lane changes (Grumert, 2018). The model distinguishes three main lane-changing types: strategic, cooperative and tactical (Erdmann, 2015). A strategic lane change is performed when the vehicle cannot continue its planned route by keeping to the current lane. This could i.e. be the case if the current lane diverts from the motorway. A cooperative lane change is performed when a vehicle is changing lane in order to facilitate another vehicle's lane changing procedure (Grumert, 2018). On a motorway, a cooperative lane change from the rightmost lane to the adjacent lane lets a parallel incoming vehicle from the on-ramp enter the motorway. Tactical lane changing on the other hand occurs when a vehicle follows vehicle with a speed that is lower than the its desired speed. The following vehicle then performs a tactical lane change to gain speed. These types of lane changes are considered when the need to gain speed outweighs the effort it takes to perform a lane change (Erdmann, 2015).

3 Methodology

In order to investigate the possible effects on traffic flow that autonomous trucks could have, microscopic traffic simulations have been used throughout this thesis. As mentioned in section , there are several microscopic simulation software available today. In this thesis, the software SUMO (Simulation of Urban Mobility) was chosen, a modelling software developed by the German Aerospace Center (German Aerospace Center, 2019c). In order to run simulations, SUMO was accompanied with several Python-files, which controlled the simulation's input and output data.

In total, three different scenarios were simulated in SUMO. Section 3.2 explains their background and structure. In the simulations, three types of autonomous trucks (AT:s) were defined. Each type of AT was characterised by a range of parameters related to the longitudinal and lateral driving behaviour. Section 3.1 describes the driver behaviour of all AT types and their relevant parameters. In section 3.3 the structure of the simulation model and its associated Python scripts are explained. Figure 3.4 summarises the information into a flowchart which shows the model structure. Lastly, section 3.4 describes the process of calibrating the simulation model based on data from Trafikverket (2019).

3.1 Defining AT driving styles

There is currently not for certain how autonomous truck will behave in real traffic situations on motorways. This uncertainty advocates testing how different driver behaviours affect traffic flow. In an interview with Tomas Olsson, at Einride, a Swedish company developing autonomous truck technology, he stated that making AT vehicles managing overtaking procedures is complicated, and will at first be avoided as much as possible. Much later in development, autonomous trucks are thought to manage overtakings and lane-changes as well as regular trucks. Calvert, Schakel and Lint (2017) argues that the deployment of cooperation between AT:s, with for instance V2V communication systems, is likely to be delayed, in comparison to lower automation systems.

The parameters that have been adjusted to define the AT driving styles are shown in table 3.1. The parameter *sigma* was set equal to 0.0 for all AT:s. *sigma* regulates the driver imperfections, in other words the likelihood of driving errors. When a fully autonomous truck gets permission to drive on public motorways, the occurrence of driving errors is assumed to have been minimised, advocating *sigma* values equal or close to 0.0. The *speedFactor* parameter defines the vehicle's desired speed in relation to the speed limit. The vehicle's desired speed is given by the *speedFactor* multiplied with the speed limit. In these simulations it was set to 1.0 and *speedDev*, which regulates the divergence from the *speedFactor*, was to 0.0 for all AT:s, since it was assumed that an autonomous vehicle will not violate the speed limit at any time.

The parameter *tau* regulates the desired time gap to a preceding vehicle. Calvert, Schakel and Lint (2017) state that several simulations with ACC-equipped vehicles have used desired gap times between 1.2 to 1.8 seconds. *tau* was set to 2.0 for the conservative AT, since AT:s will have larger breaking distances compared to smaller autonomous vehicles and thus need larger time gaps. Later in the development of autonomous technology, the AT:s are assumed to be able to handle all possible traffic situations and keep a smaller time headway to the preceding vehicle. *tau* for the aggressive driving style is reduced to 0.8 seconds, which is slightly smaller than the default value of 1.0. The cooperative AT used an even smaller time gap. Müller (2012) stated that the distance gap in a platoon could be as little as 10 meter, which in the current network corresponds to a time gap of approximately 0.5 seconds. Alipour-Fanid et al. (2017) also used a time gap of 0.5 seconds when simulating CACC vehicles and found a string of vehicles to be string stable. *tau* for the cooperative AT was thus set to 0.5 seconds.

The conservative and aggressive AT:s used a car following model developed for vehicles equipped with ACC-systems. The AT:s equipped with V2V technology instead used the CACC car-following model. Both models, which were developed by Milanés and Shladover (2014), are described in section 2.3.4 and 2.3.5.

Furthermore, there are a range of parameters associated with the lane changing behaviour. In all scenarios, the default lane changing model LC2013 was used, which is described in section 2.5.1. The parameter *lcStrategic* regulates the strategic lane changing, (German Aerospace Center, 2019a). If the parameter value is larger than the default value 1.0, the vehicles perform lane changing earlier than a default vehicle. For the conservative AT, the parameter *lcStrategic* was first adjusted to 0.8 since overtakings were to be avoided. This however, resulted in large traffic jams at intersections, due autonomous trucks changing lane very late and therefore made following vehicles break hard. *lcStrategic* was thus left at the default value 1.0. For the other two AT:s, the parameter was set to 1.2. Calvert, Schakel and Lint (2017) argued that generally, vehicles with ACC-systems are likely to perform lane changes earlier than regular drivers.

Changes to *lcSpeedGain* affects the eagerness to perform tactical lane changes to gain speed. This could for instance be the case if there is a slower vehicle ahead in the same lane. The conservative AT:s are assumed to avoid these kinds of lane-changes as much as possible and thus get a *speedGain* value of 0.0. The other AT:s will also, to a certain extent, try to avoid lane changes to gain speed, since travel time is not as critical for a freight transport as for a passenger transport. In some situations however, when the preceding vehicle's speed deviates significantly from the AT's speed, such lane changes are needed. *speedGain* is set to half the default value (see table 3.1).

lcKeepRight regulates the eagerness to keep to the right. The conservative AT was given a value of 5.0 after several simulations with different parameter values were performed. *lcAssertive* decides the time gap needed in the adjacent lane in order to perform a lane change. A value lower than 1.0 increases the desired gap, resulting in less lane changing. The conservative AT got a value of 0.5 in order to avoid lane changing in general. The aggressive AT got a value of 0.9, which means that it required slightly larger gaps compared to regular trucks. The reason for this is that even though

the vehicle would be able to perform lane changes like a regular truck, it was assumed that the required gap will be larger, since it will take all available risks associated to human driving behaviour into consideration when planning a lane change. Note that no information on the exact time gaps could be retrieved since the autonomous technology is not fully developed yet. Also for the cooperative AT, *lcAssertive* was set to 0.9. The lane changing behaviours of the aggressive and the cooperative AT were assumed to be equal.

Table 3.1: *vType* paramter values for the conservative, aggressive and cooperative AT driving styles as well as for regular trucks.

Parameter	AT_{con}	AT_{agg}	AT_{CACC}	Regular trucks	Default
sigma	0.0	0.0	0.0	0.3	0.5
lcStrategic	1.0	1.2	1.2	1.2	1.0
lcCooperative	0.5	1.0	1.0	1.2	1.0
lcSpeedGain	0.0	0.5	0.5	0.75	1.0
lcKeepRight	5.0	1.0	1.0	1.9	1.0
lcAssertive	0.5	0.9	0.9	1.0	1.0
speedFactor	1.0	1.0	1.0	1.17	1.0
speedDev	0.0	0.0	0.0	0.05	0.05
tau	2.0	0.8	0.5	2.0	1.0
carFollowModel	ACC	ACC	CACC	Krauss	Krauss

3.2 Scenarios

In order to find traffic flow effects of autonomous trucks (AT:s), three different scenarios were investigated. The scenarios try to capture different aspects of autonomous freight traffic. Below, the scenarios are described briefly before a more in-depth description in chapters 3.2.1, 3.2.2 and 3.2.3.

The first scenario (from now on called *scenario A*), aimed at investigating effects of AT:s at high but stable traffic flows. Two different driving behaviours and three market penetration rates of autonomous technology (MPR_{AT}) were simulated. Scenario A, also investigated how a potential future vehicle distribution containing both AT:s and passenger cars with V2V communication systems affected the traffic flow. Scenario B on the other hand explored the coexistence of nighttime AT traffic at low speeds and the regular traffic. According to Kristoffersson and Brenden (2018), a potential effect of the introduction of autonomous trucks is that the amount of freight traffic at night could be increased significantly, since drivers' working schedules do not need to be considered when performing the route planning. Another effect of the removal of the driver is that the travel time for an AT at night will be less critical, advocating reduced speeds, in order to save energy. Scenario B investigated how and under what circumstances such traffic would be feasible. Lastly, in scenario C, AT:s effects on the network's maximum capacity was investigated. Like in scenario A, scenario C did not

only aim at capturing the isolated effects of AT exclusively, but also to study how a future distribution of both autonomous trucks and autonomous cars would affect traffic flow.

In the future AV distribution, a significant share of both the truck fleet and passenger car fleet was made up by autonomous vehicles. The vehicle distribution is shown in figure 3.1. The distribution of AT:s was assumed to consist of both AT:s with an aggressive driving style (and without V2V communication systems) and cooperative CACC trucks. All conservative AT:s were assumed to have been phased out and replaced with AT:s with a higher levels of automation. The automation among passenger cars was assumed to lag behind that of the truck fleet. Once fully automated passenger cars are introduced on Swedish roads, they are assumed to be equipped with CACC technology, enabling them to communicate with the surrounding traffic. Another equally large share of the cars were equipped with Adaptive Cruise Control systems. These vehicles used the ACC car following model described in chapter 2.1.1, but did otherwise have the same characteristics as regular cars. The resulting car share consisted of manual (regular) cars. In cars equipped with Adaptive Cruise Control, the driver is free to set any desired speed that the vehicle then tries to keep. The $speedFactor$ parameter was therefore set equal to that of regular vehicles. The parameter $speedDev$, which regulates the deviation from $speedFactor$ is, however, set to 0 since the ACC system is able to keep a smooth longitudinal driving style without deviating from the desired speed.

Fully automated and connective cars (CACC) make up a total of 20.7 % of the whole vehicle flow. Semi-automated cars (cars with Adaptive Cruise Control) make up another 20.7 %, which means that 50 % of all cars will be equipped with some type of automation technology. The truck fleet on the other hand will consist of 50 % fully automated trucks and 50 % regular trucks (see figure 3.1).

3.2.1 Scenario A (Driver behaviour)

Scenario A had two main goals. Firstly, it investigated how two types of AT driving styles without V2V communication systems affected traffic flow. As mentioned above, non-cooperative AT:s are likely to dominate the AT fleet in early stages in development. Therefore, the need for investigating how the driving styles of these vehicles affect traffic, is of great importance. Note that in order to isolate the effects of the AT:s, all passenger cars were modelled as manual non-autonomous vehicles. Secondly, scenario A investigated how a potential future vehicle distribution of both autonomous trucks and autonomous cars could affect traffic flow.

Table 3.2 shows the structure of the scenario. First two AT driving styles (conservative and aggressive) and three AT market penetration rates was combined, resulting in six different simulation combinations (A1 to A6). The last simulation (A7) aimed at capturing the effects of a potential future vehicle distribution according to figure 3.1. The AT market penetration rate is set to 50 %, which means that 50 % of all trucks used some level of automation. Among these trucks one share (corresponding to 30

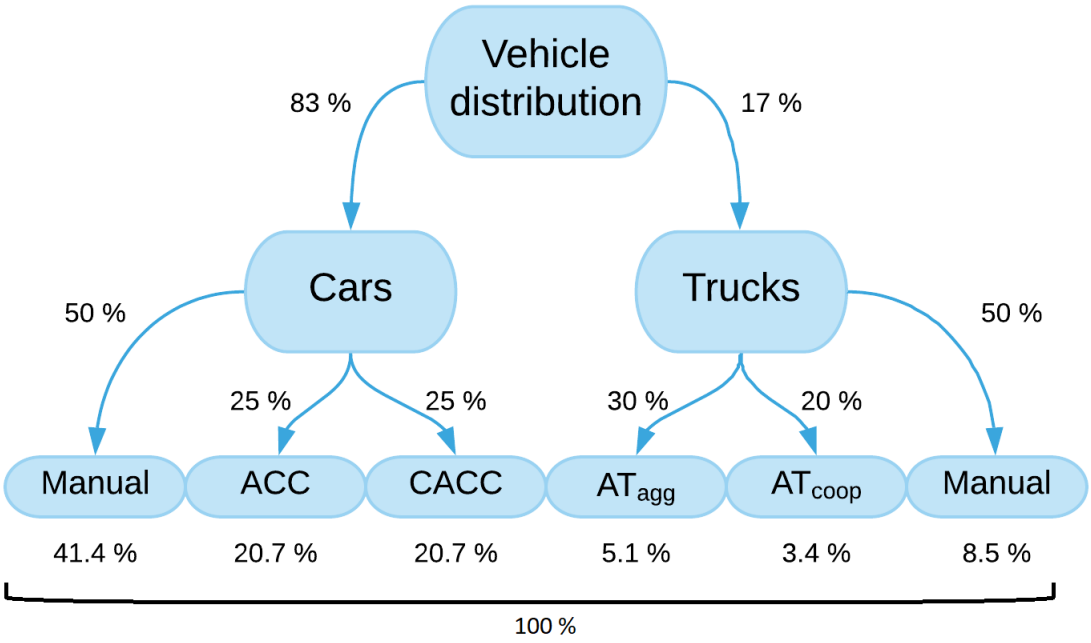

Figure 3.1: Vehicle types in the future vehicle distribution.

% of the total truck fleet) consisted of AT:s with an "aggressive" driving style. The resulting AT:s (20 % of the total truck fleet) consisted of cooperative AT:s with V2V-communication systems which enables them to form platoons. 50 % of the total truck fleet was made up by manual (regular) trucks. In each simulation, the average speed $\bar{v}$, average travel time TT and total travel cost TC, was measured. Each result was then be compared to results from a simulation without autonomous trucks.

The data for calculation of travel costs was gathered from ASEK (2016). On the part of motorway E6 that was investigated in this thesis, the amount of work commuters are high during the morning- and afternoon hours. A result is that the average valuation of travel time is relatively high. When approximating the shares of commuter trips, regular car trips and the flow of freight vehicles, the average value of time (VoT) was 144 SEK per hour. The calculations of VoT based on data from ASEK (2016), is shown in Appendix A.1.

3.2.2 Scenario B (Night driving)

In scenario B, the impact of AT truck with low speeds at night was investigated. An advantage of AT trucks is that no driver is needed to bring the freight from one place to another. Apart from economical impacts that this could have, removing the driver also affects the planning of driver schedules. As no working hours have to be considered, the time-of-day is no longer a constraint in the schedule planning process. Another effect is that the total running time for a freight vehicle is not as critical without a driver, advocating driving at lower speeds to save energy. If parts of the autonomous truck traffic shifted from day to night, and drove at significantly lower speeds, it could both make use of the free capacity available at night and the same time save energy.

Table 3.2: Simulations in scenario A (Driver behaviour).

AT driving style	Penetration rate	Simulation	Parameters
Passive	50 %	A1	$\bar{v}$, TT, TC
	75 %	A2	$\bar{v}$, TT, TC
	100 %	A3	$\bar{v}$, TT, TC
Aggressive	50 %	A4	$\bar{v}$, TT, TC
	75 %	A5	$\bar{v}$, TT, TC
	100 %	A6	$\bar{v}$, TT, TC
Mix	50 %	A7	$\bar{v}$, TT, TC

Table 3.3: Simulations in scenario B (Night driving).

Traffic flow	AT speed	Penetration rate = 50 %	Penetration rate = 100 %
300	30	Simulation B1	Simulation B2
	40	Simulation B3	Simulation B4
	50	Simulation B5	Simulation B6
500	30	Simulation B7	Simulation B8
	40	Simulation B9	Simulation B10
	50	Simulation B11	Simulation B12
700	30	Simulation B13	Simulation B14
	40	Simulation B15	Simulation B16
	50	Simulation B17	Simulation B18

Furthermore, by doing so, the traffic flow in peak hours would decrease, enabling a more stable traffic flow and lowering the risk of traffic flow breakdown. Driving at low speeds at night is however, not feasible without having knowledge about the traffic implications it could have. This scenario investigates both effects on traffic flow and on the total amounts of CO_2 emissions and tries to answer if and when this sort of traffic is suitable.

In figure 3.2, the share of freight and car traffic is shown. The data was gathered from the northbound lanes of motorway E6 in Kallebäck intersection in Gothenburg, Sweden, during an average weekday (Trafikverket, 2019). The intersection is located directly south of the motorway section modelled in this thesis and was assumed to have similar traffic flows. The car flow shows clear peaks in the morning and evening. The flow of freight vehicles does not show the same pattern. The freight flow is more evenly distributed throughout the day (See figure 3.2). However, it adds to the maximum flow in the peaks, resulting in short periods with very high flow, reaching the road capacity. At night, however, the total flow passing the Trafikverket data source is only about 5 - 15% of the flow during the morning peak (Trafikverket, 2019). If this free capacity could be used more effectively by trucks, the maximum flow in the morning-

and afternoon peaks would decrease. This would also increase the share of cars in the peak, resulting in a more homogeneous flow, which would increase traffic flow stability.

Since introducing slow autonomous trucks at night would decrease the average travel time, aggregating the travel time for each vehicle into a mean travel time is not a suitable measurement of traffic implications in this scenario. In SUMO, the parameter *timeLoss* was instead chosen as as an indicator of the effects. It shows the average difference between a vehicle's actual travel time and the vehicle's minimum travel time, given ideal circumstances, such as free flow without being hindered by surrounding traffic (German Aerospace Center, 2019b).

In the simulations, three AT speeds, two AT penetration rates and three different vehicle flows werw considered. The AT vehicle speed is set to either 30, 40 or 50 km/h, whereas the penetration rate is set to either 50 % or 100 %. The traffic flow levels were based on data from the Trafikverket loop detector at Gårda intersection (see figure 1.1). At the data source, the traffic flow at night varied between 100 and 400 vehicles per hour. Around 03:00 in the morning the traffic flow started to increase rapidly, reaching the morning peak flow of around 4000 vehicles per hour at 07:30. The fast increase in traffic flow in the morning hours advocates the need to consider different traffic flows. The traffic flow was therefore either set to 300, 500 or 700 vehicles per hour, resulting in 18 different simulation combinations. Every combination was simulated 10 times, after which the mean *timeLoss* value was calculated. Note that even the lowest traffic flow at 300 veh/h is higher than the lowest recorded flow from the data source. The reason for this is that there could be seasonal variations in the traffic flow data that was not shown in the studied data sample. If that were to be the case, the model results should be valid for such a traffic flow. If the flows on the motorway were kept much lower than the input flows in the simulation, the simulation results would be slightly exaggerated compared to reality.

The parameter *timeLoss* increases as the traffic flow increases, since more traffic means that all vehicles need to adjust their driver behaviour to surrounding traffic. To isolate the impact of the introduction of AT trucks, the simulation was first run 10 times without AT vehicles. This generated a base *timeLoss* value, which was subtracted from all other simulation results, giving the average increase in travel time during each simulation. The structure of scenario B is shown in table 3.3. The simulation results can be seen in table 4.4, 4.5 and 4.6 in chapter 4.2.

3.2.3 Scenario C (Capacity)

In scenario C, effects on the road capacity was investigated. The number of vehicles entering the model was increased linearly throughout the simulation, making the traffic flow reach capacity. The traffic flow characteristics were investigated in two main ways. Firstly, loop detectors were placed 100 meters south of the on-ramp, measuring aggregated parameters such as average vehicle flow and average speed for vehicles that have passed the detector every minute. The speed and flow data was then plotted in a

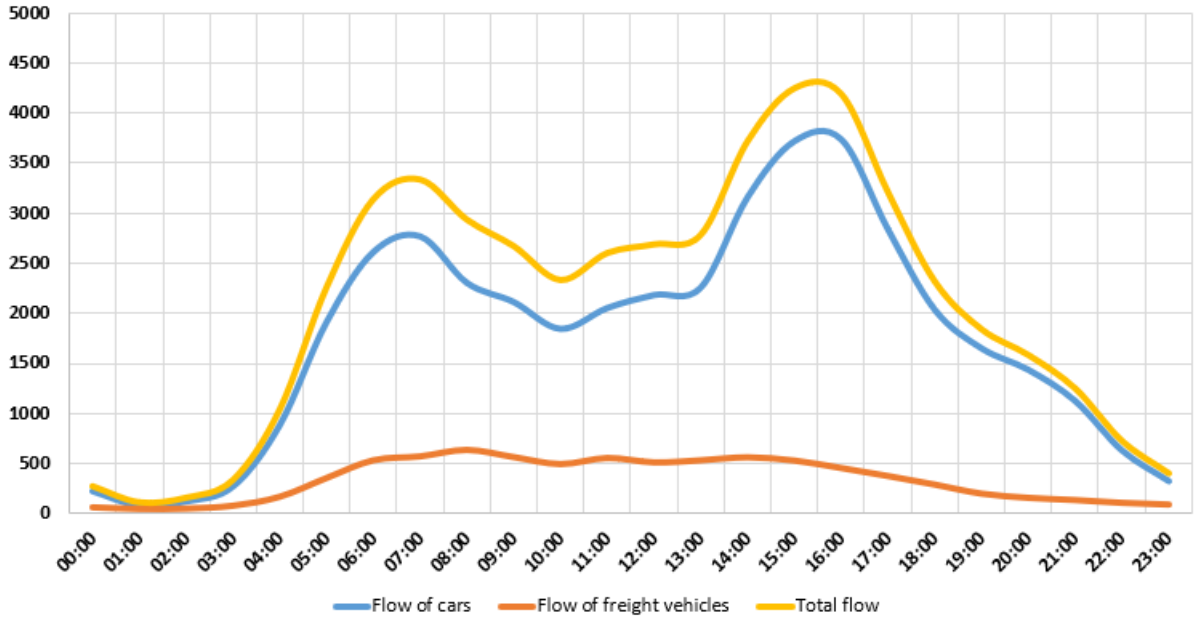

Figure 3.2: Flow of freight and car traffic on motorway E6 at Kallebäck intersection, october 2019. Source: Trafikverket (2019)

diagram which showed the maximum flow that had been reached at detectors in lane 1, 2 and 3. Secondly, data was gathered on a microscopic level to get a more detailed picture of the vehicle speeds in the whole network. Once every second the speed and travelled distance was gathered from all passing vehicles. This data was then plotted in a trajectory diagram, which showed where and when congestion emerges in the network, as well as the length of the congested string of vehicles.

Table 3.4 shows the structure of all simulations in scenario C. Similar to scenario A, two types of driver behaviours and a future vehicle distribution was simulated separately. Three levels of MPR_{AT} was used, resulting in seven different simulations. Each simulation is run three times with different random seeds.

Table 3.4: Simulations in scenario C (Capacity).

AT driving style	Penetration rate	Simulation	Parameters
Passive	50 %	C1	$\bar{v}$, Breakdown flow
	75 %	C2	$\bar{v}$, Breakdown flow
	100 %	C3	$\bar{v}$, Breakdown flow
Aggressive	50 %	C4	$\bar{v}$, Breakdown flow
	75 %	C5	$\bar{v}$, Breakdown flow
	100 %	C6	$\bar{v}$, Breakdown flow
Future vehicle distribution	50 %	C7	$\bar{v}$, Breakdown flow

3.3 Model description

In figure 3.4 the structure of the simulation model is shown. In a first step the network file was created, in which the traffic network is defined with nodes and edges. The traffic network was created with a software called NetEdit, a separate tool for creating and modifying networks used specifically in SUMO simulations. The network was made to resemble Ullevi and Örgryte intersections along the motorway E6 in Gothenburg, Sweden. The model contains five possible routes for vehicles to take (see figure 3.3). Note the location of the loop detector from which data was gathered. The network was then saved in a (*.net*) file.

Next, traffic that would run through the network had to be defined. Each vehicle type got its vehicle and driver characteristics by setting a large range of parameter values. In table 3.5, available vehicle parameters and their default values are shown. Depending on the choice of car-following model and lane-changing model, there are several additional parameters that can be adjusted. Table 3.6 shows available car-following parameters and table 3.7 shows parameters related to the choice of lane-changing model.

In this model four vehicle categories were used: passenger vehicles (cars), light trucks, trucks with semitrailers and trucks with trailers. The vehicle categories were based on data from Trafikverket (2019) collected from the northbound lanes on motorway E6, north of Örgryte intersection in Gothenburg, 2019. The detectors registered average flows and average vehicle lengths every minute during 24 hours. A few average vehicle lengths that is currently not allowed on Swedish roads were registered. These measurements were seen as errors and were thus excluded. From the remaining data, the above mentioned vehicle categories were defined. The length of the passenger vehicle was approximated to 3 to 5 meters, the light truck to 9.5 meters, the semitrailer truck to 16.5 meters and the truck with trailer to 20 meters.

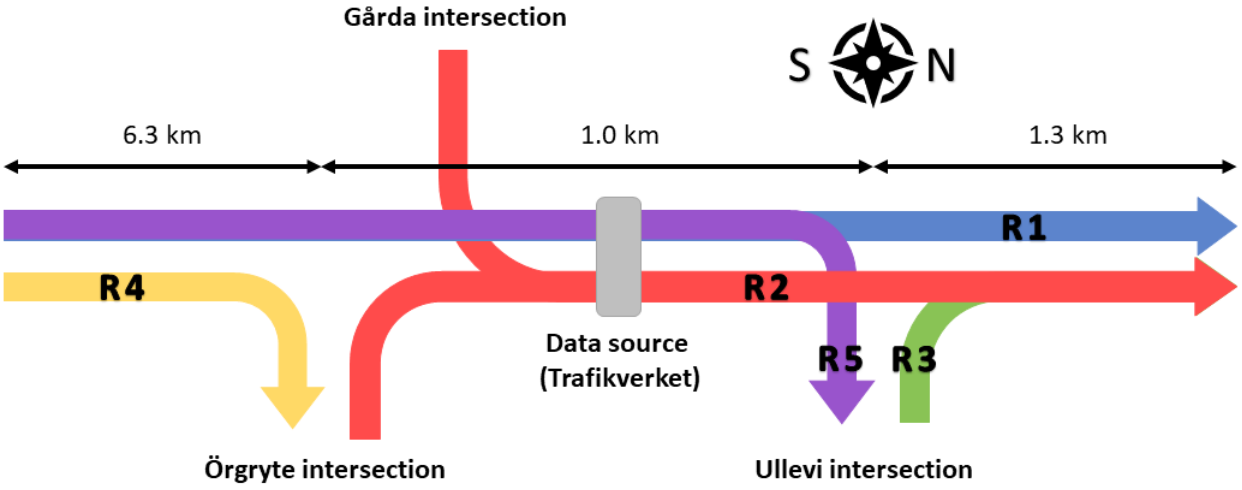

Figure 3.3: Routes in the simulation model.

Table 3.5: Available vehicle type parameters that can be adjusted. Source: German Aerospace Center (2019a)

Headway type	Default	Regulates
accel	2.6	Vehicle acceleration
decel	4.5	Vehicle deceleration
length	5.0	Vehicle length
minGap	2.5	Minimal gap to leading vehicle [m]
speedFactor	1.0	Adjusts vehicles' desired maximum speed
speedDev	0.1	Deviation from speedFactor
color	yellow	Vehicle color
width	1.8	Vehicle width
carFollowModel	Krauss	Car-following model
laneChangeModel	LC2013	Lane changing model

Table 3.6: Parameters specific for the Krauss and IDM cal-following models. Source: German Aerospace Center (2019a)

Headway type	Default	Regulates	Car-following model
sigma	0.5	Driver imperfection	Krauss, IDM
tau	1.0	Desired time headway	All models
delta	4.0	Acceleration exponent	IDM
stepping	0.25	Step length when computing follow speed	IDM

Table 3.7: Parameters specific to the LC2013 lane changing model. Source: German Aerospace Center (2019a)

Headway type	Default	Regulates
lcStrategic	1.0	Eagerness to perform strategic lane changing
lcCooperative	1.0	Eagerness to perform cooperative lane changing
lcSpeedGain	1.0	Eagerness to perform lane changing to gain speed
lcKeepRight	1.0	Eagerness to keep right
lcOvertakeRight	0	Probability to overtake on the right
lcOpposite	1.0	Eagerness for overtaking via the opposite-direction lane
lcAssertive	1.0	Willingness to accept smaller gaps in the target lane

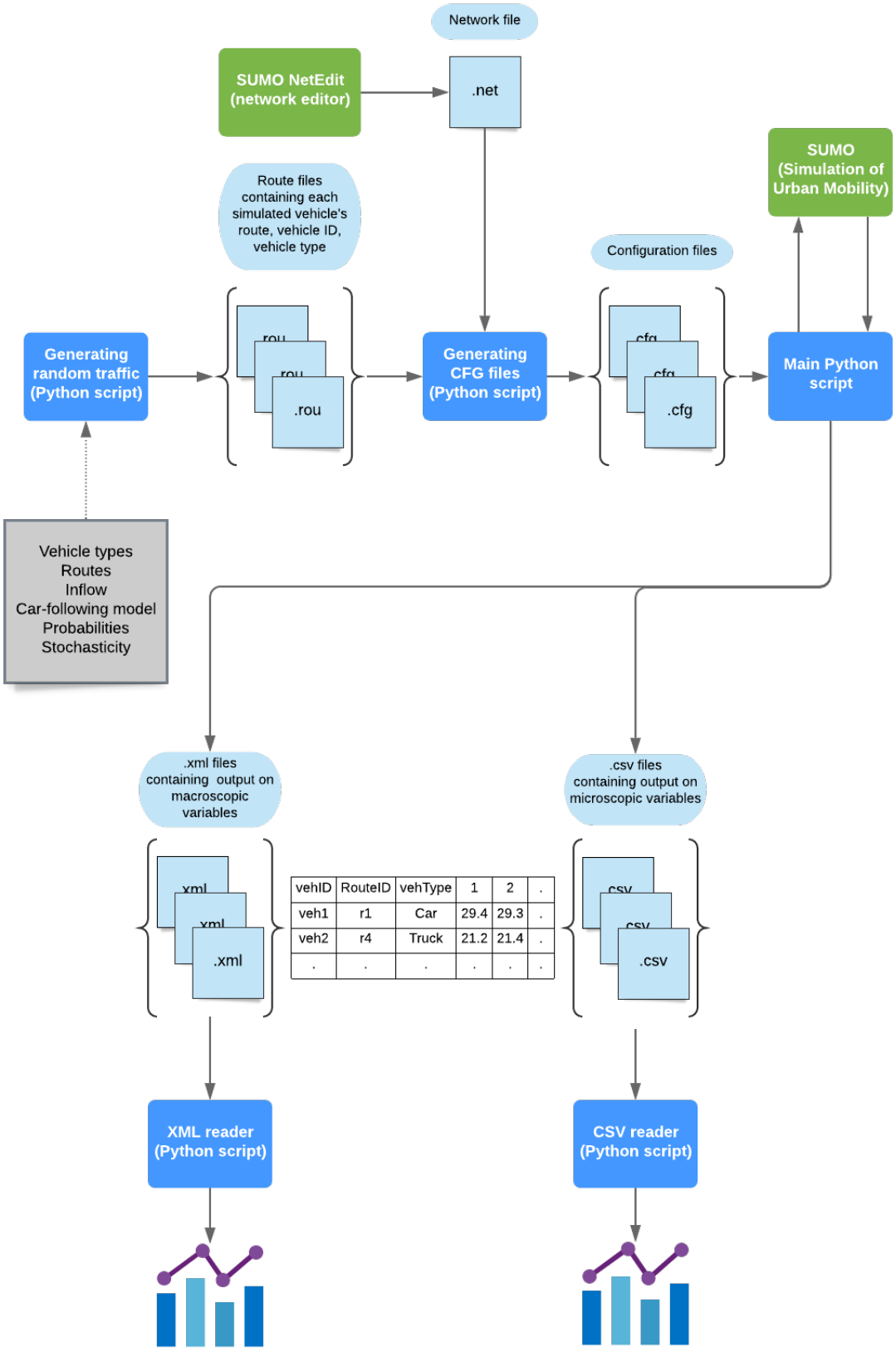

Figure 3.4: Structure of the Python-scripts, controlling the simulations.

3.3.1 Traffic generation

In SUMO, vehicle and driver characteristics are defined in a route file (*.rou.xml*) (German Aerospace Center, 2019a). In a route file, the type of vehicles (vehicle characteristics and driving behaviour) and each vehicle's route in the network has to be specified. A vehicle type, e.g. passenger car or a truck is defined by a string of .xml code starting with `vType`:

```
'<vType vClass="passenger" accel="2.9" decel="4.5" id="Car"
length="4.5" maxSpeed="40" sigma="0.5"/>'
```

```
'<vType vClass="trailer" accel="1.4" decel="3.5" id="Truck"
length="16.0" maxSpeed="22.22" sigma="0.1"/>'
```

On the stretch of motorway between Öregryte and Ullevi intersections, the flow of passenger cars is dominant and thus affecting the flow characteristics the most. In order to resemble heterogeneous traffic with a wide range of vehicles and make the flow of vehicles less deterministic, a number of passenger vehicle types were used, each with parameters generated from stochastic variables. In Python, a for-loop is used to generate 100 different passenger vehicle types. In each iteration, parameters are given unique values, resulting in range of vehicle characteristics and driver behaviours. More information about the stochastic distributions that were used can be seen in table 3.10.

When defining the freight vehicle types, three vehicle types are created: *Light truck*, *Truck with semitrailer* and *Truck with trailer*. In peak, the flow of freight vehicles is relatively low. As a result, small variances in driver behaviour of freight vehicles were assumed to have a limited effect on the overall traffic flow. For this reason, all freight *vType* parameters are given definite values.

From the vehicle types, singe vehicles were created. Apart from the vehicle type characteristics, a single vehicle needs a route to travel on in the network as well as information about choice of car-following model and lane-changing model. The network contains five possible routes, which are shown in figure 3.3. Continuous data from the Trafikverket detector close to Gårda intersection, together with data from on- and off ramps were used to approximate the flow on each route in the model. When assigning a route to a vehicle, the route is chosen by a discrete random variable, with probabilites resembling the approximated route flows.

3.4 Calibration procedure

In order to resemble the traffic through Ullevi and Örgryte intersections, the model had to be calibrated. A manual calibration procedure was used to tune parameters against loop detector data, provided by the Swedish Transport Administration (Trafikverket, 2019). The data was gathered from detectors that continuously collected data on traffic flow, average headways, vehicle lengths and speeds per lane during a 24-hour period. Since the traffic flow was dominantly made up of passenger cars, the data

Table 3.8: Passenger car parameters in the calibration.

Parameter	Regulates
tau	Desired time headway
sigma	Driver imperfection
speedFactor	Drivers' violation of the speed limit
speedDev	Deviation from the *speedFactor*
lcStrategic	Eagerness to perform strategic lane changing
lcCooperative	Eagerness to perform cooperative lane changing
lcSpeedGain	Eagerness to perform lane changing to gain speed
lcKeepRight	Eagerness to keep right
lcAssertive	Willingness to accept smaller gaps in the target lane

Table 3.9: Freight parameters in the calibration.

Parameter	Regulates
lcStrategic	Eagerness to perform strategic lane changing
lcCooperative	Eagerness to perform cooperative lane changing
lcSpeedGain	Eagerness to perform lane changing to gain speed
lcKeepRight	Eagerness to keep right
lcAssertive	Willingness to accept smaller gaps in the target lane

from the detectors could not be used to calibrate freight car-following parameters. The values of these parameters were therefore been gathered from other sources. The freight lane-changing parameters however, were included in the calibration. Below the three categories of parameters in the calibrations are shown.

- Passenger car-following parameters
- Passenger lane-changing parameters
- Freight lane-changing parameters

Hollander and R. Liu (2008) describe the general procedure of calibrating micro simulation models. According to the authors, available parameters have to be categorised in order to detect the ones that are subject to calibration. Parameters, whose values can be determined from other sources, e.g. vehicle characteristics, should be excluded from the process. Also, if reliable parameter values can be obtained from other similar micro simulations, these are then not subject to calibration. Furthermore, only parameters which have a significant effect on traffic flow should be included (Hollander and R. Liu, 2008).

Based on this information, only the parameters shown in table 3.8 were found subject to calibration. The resulting parameters were either gathered from data, from previous research or could not be calibrated with the provided data. These parameters were therefore excluded. For instance, the lane-changing parameters *lcOpposite* and *lcOvertakeRight* were excluded from the calibration procedure. The road network

studied in this thesis is a motorway with median dividers and grade separated intersections. The parameter *lcOpposite* regulates overtakings in the opposite-direction lane, and was therefore not relevant in this case. Also *lcOvertakeRight*, which regulates the probability of overtaking another vehicle on the right were excluded, since no data had been collected that could show this behaviour.

The provided data from Trafikverket (2019), showed information on flow, average headways and average speeds. The aim of the calibration was to minimise the mean squared standard error (RMSE) between this data and the simulated vehicle flows, average headways and average speeds.

3.4.1 Parameter values prior to calibration

Before the actual calibration procedure started, all calibration parameters were given initial values. Bjärkvik et al., 2017 calibrated a SUMO traffic simulation model based on data from the Drive Me route - a route around central Gothenburg that was used to test autonomous vehicles in mixed traffic. The route consists mostly of urban motorways with 2 or three lanes in each direction and incorporates the motorway section investigated in this thesis. The car traffic through Gårda and Ullevi intersections were therefore assumed to be similar to the traffic on the Drive Me Route. Some parameter values from the Drive Me model were therefore used as initial values before the calibration procedure.

Bjärkvik et al. (2017) found that the desired time headway, *tau*, followed a log-normal distribution with mean $\mu = 0$ and standard deviation $\sigma = \sqrt{0.4}$ on the Drive Me route. Based on this this, *tau* was assumed to be log-normally distributed also in this model. The value of σ,and μ however, were not known and was investigated during the model calibration.

Some further parameter values were gathered from the work of Bjärkvik et al. (2017). The minimum gap to the preceding vehicle at standstill, *minGap* was assumed to follow a Gamma distribution with shape parameter $k = 0$ and scale parameter $\theta = 1.0$. The vehicles acceleration ability, *accel*, was set to follow a uniform distribution between 2.7 and 3.3 m/s^2 and the deceleration ability was set to 4.5 m/s^2. Lastly, the *impatience* parameter, regulating the driving behaviour if the vehicle has to halt unintentionally, was set to 0.5 (Bjärkvik et al., 2017).

Some parameters were approximated from other external sources. The vehicle length, *length*, was assumed to vary between 4 and 5 meters, covering the default vehicle lengths of passenger cars and passenger vans used in SUMO (German Aerospace Center, 2019d). In the *vType* code, *length* was generated from a uniform stochastic parameter varying between 4 and 5 meters.

The driver imperfection *sigma* was initially set to the default value 0.5. The drivers' actual mean speed, given by the *speedFactor* parameter, was approximated from data provided by the Swedish Transport Administration (Trafikverket, 2019). Detectors on each of the three northbound lanes between Örgryte and Ullevi intersections collected data on average speeds every minute for 24 hours during a weekday in November 2019.

The *speedFactor* parameter was approximated by dividing the average speed during each minute with the speed limit. The distribution of the *speedFactor* parameter for passenger cars can be seen in figure 3.5. The distribution that fit the data the best was a normal distribution with mean $\mu = 1.2$ and a standard deviation $\sigma = 0.2$. For freight vehicles *speedFactor* was normally distributed with $\mu = 1.17$ and $\sigma = 0.11$. Both μ and σ was adjusted in the calibration.

The *speedDev* parameter, which regulates the deviation from the *speedFactor* was set to 0 in prior to the calibration, since it was assumed that enough variation in speeds was captured by the distribution of the *speedFactor*. During calibration it was investigated whether this hypothesis held true. This was also the case for the remaining parameters *width*, *carFollowModel*, *laneChangeModel*, *lcStrategic*, *lcCooperative*, *lcSpeedGain*, *lcKeepRight* and *lcAssertive*. Default values were initially used, but later adjusted during the calibration.

In table 3.11 the freight car-following parameters are shown. The acceleration ability *accel* and deceleration ability *decel* were set to SUMO's default values for light trucks, trucks with semitrailers and trucks with trailers. The speed deviation *speedDev* was set to the default value for freight vehicles, 0.05 (German Aerospace Center, 2019d). The driver imperfection *sigma* was set to 0.3, slightly lower than for passenger cars, since it was assumed that truck drivers have more routine and driving skills than average regular car drivers. The parameter *impatience* was set to 0 since it was assumed that travel times are not as crucial during a freight journey as it is for morning car commuters (see ASEK (2016)). The resulting car-following parameters were set to default values. Also, all lane-changing parameters were set to the default value 1.0 in prior to the calibration.

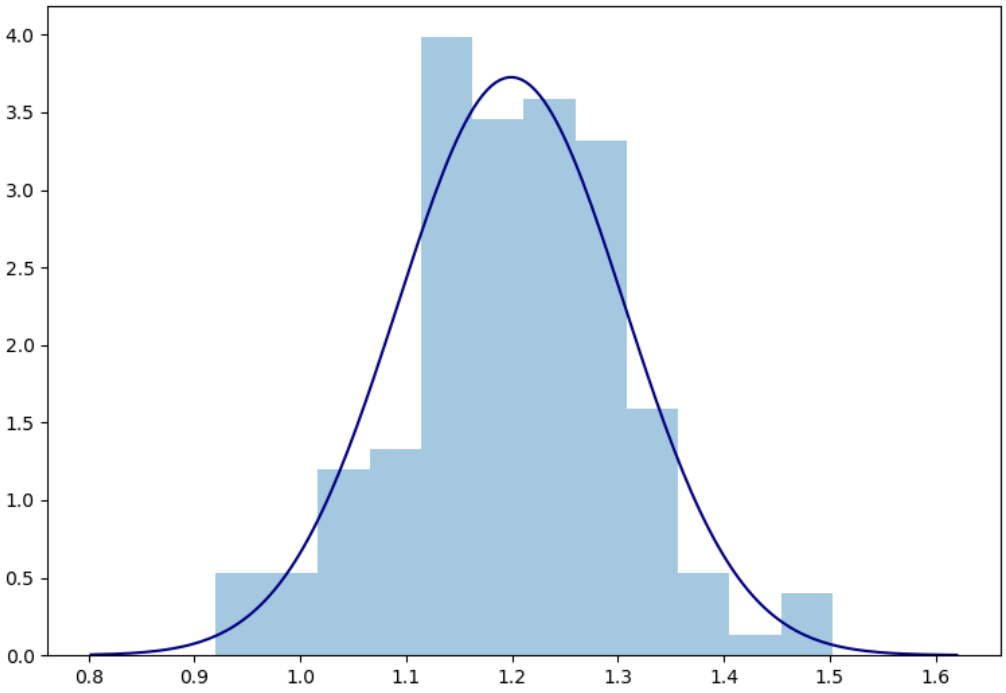

Figure 3.5: Distributions of speed factors for passenger cars in the northbound lanes on E6 motorway, north of Örgryte intersection, Gothenburg. Normal distribution with $\mu = 1.2$ and $\sigma = 0.2$.

Table 3.10: Parameters for cars before calibration.

Parameter	Value/Distribution	Unit	In calibration?
accel	$U(2.7, 3.3)$	m/s^2	No
decel	$U(6.5, 7.5)$	m/s^2	No
length	$U(4.0, 5.0)$	m	No
impatience	0.5		No
minGap	$Gamma(0.0, 1.0)$	m	No
maxSpeed	40	m/s	No
width	1.8	m	No
carFollowModel	Krauss		No
laneChangeModel	LC2013		No
tau	$Lognormal(0.0, 0.4)$	m	Yes
sigma	0.5		Yes
speedFactor	$N(1.2, 0.1)$		Yes
speedDev	0.1	m/s	Yes
lcStrategic	1.0		Yes
lcCooperative	1.0		Yes
lcSpeedGain	1.0		Yes
lcKeepRight	1.0		Yes
lcAssertive	1.0		Yes

Table 3.11: Parameters for freight vehicles before calibration.

Parameter	Light truck	Semitrailer	Trailer	In calibration?
accel	1.3	1.1	1.0	No
decel	4.5	4.5	4.5	No
length	9.5	16.5	20.0	No
tau	1.0	1.0	1.0	No
minGap	2.5	2.5	2.5	No
sigma	0.3	0.3	0.3	No
impatience	0	0	0	No
speedFactor	1.0	1.0	1.0	No
speedDev	0.05	0.05	0.05	No
maxSpeed	22.22	22.22	22.22	No
width	2.55	2.55	2.55	No
carFollowModel	Krauss	Krauss	Krauss	No
laneChangeModel	LC2013	LC2013	LC2013	No
lcStrategic	1.0	1.0	1.0	Yes
lcCooperative	1.0	1.0	1.0	Yes
lcSpeedGain	1.0	1.0	1.0	Yes
lcKeepRight	1.0	1.0	1.0	Yes
lcAssertive	1.0	1.0	1.0	Yes

3.4.2 Calibrating flows

All parameters suited for calibration are shown in table 3.8. In the first step, the flows of vehicle types in all lanes are investigated. Data from Trafikverket (Trafikverket, 2019) show approximate vehicle distributions in each of the northbound lanes. By manually changing the lane changing parameters in table 3.8, a vehicle distribution in the simulation was reached that matched the data well. Table 3.12 below shows the parameter values in combination with the output vehicle distribution.

Table 3.12: Calibrated lane changing parameters.

Parameter	Car	Light truck	Semitrailer	Trailer
lcStrategic	0.8	0.7	0.7	0.7
lcCooperative	1.3	1.2	1.2	1.2
lcSpeedGain	1	0.75	0.75	0.75
lcKeepRight	1	1.9	1.9	1.9
lcAssertive	1	1	1	1
Flow lane 1 [%]	75	16	2	6
Simulated flow lane 1 [%]	78	13	1	8
Flow lane 2 [%]	84	12	1	3
Simulated flow lane 2 [%]	90	6	2	3
Flow lane 3 [%]	91	8	0	1
Simulated flow lane 3 [%]	93	5	0	2

3.4.3 Calibrating speeds

After the lane changing parameters had been calibrated and the simulation output showed accurate flows in each lane, the car-following parameters regulating speed, *speedFactor* and *speedDev* for the passenger vehicles were adjusted. By investigating the data on average speeds from the loop detector at Gårda intersection, it was found that cars' deviations from the speed limit could be approximated to a log-normal distribution with $\mu = 1.2$ and $\sigma = 0.2$ (see figure 3.5). For freight vehicles the deviation was normally distributed with $\mu = 1.17$ and $\sigma = 0.11$. It was not for certain however, that these settings were the ones that would generate simulation outputs that matched the speed data the best after the lane-changing parameters had been changed. Since the car traffic is dominant on the investigated route, *speedFactor* and *speedDev* for the passenger vehicles are adjusted, whereas values for the freight vehicles remained the same. In section 3.4.1, a hypothesis was that *speedDev* could be set equal to zero because by letting the *speedFactor* parameter follow a stochastic distribution, the standard deviation σ would capture the deviations from the speed limit. By simulating combinations of *speedFactor* and *speedDev* one could show whether this hypothesis held true.

	$\mu = 1.2$		
speedDev	$\sigma = 0.05$	$\sigma = 0.10$	$\sigma = 0.15$
0.0	1.7	1.54	1.82
0.05	1.58	1.48	1.64
0.1	1.53	1.78	1.89

Table 3.13: Mean square errors for combinations of *speedFactor* and *speedDev*.

Nine combinations were simulated, generating average speeds that were compared with speed data from Trafikverket (2019). The aim of the *speedFactor* and *speedDev* calibration was to minimise the mean square error between the simulation output and the data. The results are shown in table 3.13. The μ parameter of *speedFactor* was varied but $\mu = 1.2$ turned out to generate the best fit. Table 3.13 therefore only shows the calibration results with this value of μ. Each combination was simulated ten times. $speedFactor = Lognorm(1.2, 0.1)$ together with *speedDev*=0.05 generates the best fit to the data. The results therefore differ slightly from the initial approximations of *speedFactor* and *speedDev*.

3.4.4 Calibrating headways

In the next step, parameters affecting headways were calibrated. The car-following parameters *tau* and *sigma* were assumed to affect the average headways in each lane. When experimenting with random combinations of these parameters however, *sigma* turned out to have no significant effect on the average simulated headways. Therefore, only *tau* were calibrated againts the headway data. Bjärkvik et al. (2017) found that *tau* was log-normally distributed on the DriveMe route in Gotheburg. In these simulations, *tau* was therefore assumed to follow a log-normal distribution but with unknown parameters. Combinations of means and standard deviations were therefore simulated in order to find which log-normal distribution that fitted the data from Trafikverket (2019) the best. Every combination was simulated five times. The parameter combination that minimised the summarised square root mean error compared to the data was thereafter chosen. Table 3.14, shows the mean square errors when running simulations with different *tau* distributions. A log-normal distribution with $\mu = -0.2$ and $\sigma = 0.6$ generated the best fit (see table 3.14).

σ	$\mu = -0.2$	$\mu = 0.0$	$\mu = 0.2$	$\mu = 0.4$	$\mu = 0.6$
0.2	2.54	2.60	2.60	2.62	2.65
0.4	2.56	2.79	2.58	2.64	2.67
0.6	2.45	2.94	2.72	2.72	2.65
0.8	2.92	3.09	2.76	2.93	2.74

Table 3.14: Headway mean square errors for different log-normal distributions of *tau*.

4 Results

In this section, the results from the simulations are presented. The results from each scenario are compared to simulation results from base scenarios, without autonomous vehicles, in order to analyse the effects. The results refer to simulation numbers, which can be found in tables 3.2.1, 3.2.2 and 3.2.3.

4.1 Results from scenario A

4.1.1 Travel times

In table 4.1 the average increase in travel time per vehicle is shown. The parameter *timeLoss* has been used to find the travel time increases. *timeLoss* measures the difference between a vehicle's actual travel time and its *ideal* travel time if it continuously drove with its desired speed. For each combination of driver behaviour type and penetration rate, a two-tailed t-test shows if the mean *timeLoss* value differs significantly from the base simulation. The null hypothesis (H_0) is that the *timeLoss* mean from simulation i is equal to the mean from the base simulation (see formula 4.1). If the null hypothesis is true, there is no significant difference between the mean of the simulation output and the results from the base simulation. The significance level is set to 0.05.

$$H_0 : \mu_{base} - \mu_i = 0 \tag{4.1}$$

The increase in travel time was measured along a 3.3 km long section of the motorway, which included the on-ramps in Örgryte and Ullevi intersections. Table 4.1 both shows the total increase in travel time and the travel time increase per kilometre. An increased travel time affects the travel costs for all vehicles travelling through the network. Table 4.2 shows the change in total travel costs (TTC), related to the car drivers' and the freight vehicles' VoT.

The conservative driving style generated *timeLoss* values that differed significantly from the base simulation. The null hypothesis was rejected for all market penetration rates and the difference in *timeLoss* compared to the base scenario increased with an increasing MPR_{AT} (see table 4.1). Despite significant change compared to the base simulation, the total travel time increases are small. In the base simulation the average travel time through the 3.3 km long motorway section was 59.5 seconds. This means that the increase in travel time ranged between 0.87 % and 2.53 %, when simulating the conservative driving style. The aggressive driving style generated even smaller travel time increases. At a MPR_{AT} of 50 %, the change in *timeLoss* was insignificant at a significance level of 0.05, which means that H_0 could not be rejected. A MPR_{AT}

Table 4.1: Increase of average travel times when introducing AT vehicles in scenario A. Traffic flow = 3500 veh/h.

	Passive			Aggressive			Mix
	50 %	75 %	100 %	50 %	75 %	100 %	50 %
Mean *timeLoss* increase [s]	1.71	2.59	4.96	0.21	0.84	0.42	6.73
Mean *timeLoss* increase [s/veh km]	0.87 %	1.32%	2.53 %	0.11 %	0.43 %	0.21 %	3.43 %
p-value	0.03	0.02	<0.01	0.72	0.33	0.59	<0.01
Reject H_0?	Yes	Yes	Yes	No	No	No	Yes

Table 4.2: Increase in total travel costs [SEK/km*h] when introducing AT vehicles in scenario A. Traffic flow = 3500 veh/h.

Passive			Aggressive			Mix
50 %	75 %	100 %	50 %	75 %	100 %	50 %
72	109	210	9	36	18	284

of 50 % and 75 % generated small, yet significant changes to *timeLoss*. In contrast to the conservative driving style, an increasing MPR_{AT} of aggressive AT:s did not generate larger *timeLoss* values (see table 4.1). The relatively large *timeLoss* values for the conservative driving style could be partly explained by their lane changing behaviour. The conservative AT:s try to avoid lane changes as far as possible. The trucks therefore keep to the rightmost lane, forcing the surrounding traffic to perform many lane changes in order to overtake the AT:s. This behaviour is shown in figure 4.3.

Table 4.1 also shows the increase in travel times when simulating an assumed future vehicle distribution according to section 3.2. The travel time increased with 6.73 seconds, which corresponds to approximately 2 seconds per vehicle-kilometre and a travel time increase of 3.4 %. The relatively large increase in travel time relates to the increase of vehicles that do not deviate from the speed limit. In the future vehicle distribution, automation is introduced within the passenger car fleet. The autonomous cars have, like the AT:s, a *speedFactor* of 1.0, which means that their desired speed equals the speed limit. Their speed, however, deviates from the average speed, since the regular cars and trucks have desired speed that are larger than the speed limit. Consequensively, the non-autonomous vehicles are hindered from driving at their desired speeds, which increases the *timeLoss* parameter. In order to investigate this theory, a few simulations were carried out after changing the *speedFactor* settings for the non-autonomous cars. When setting *speedFactor* equal to 1.0, the average *timeLoss* value dropped to -0.6 %. The AT:s thus affect the average travel times negatively, but the negative impact is due to the surrounding manual vehicles not keeping

the speed limit.

Table 4.2 shows how the total travel costs are affected by the changes in travel time. The travel costs are approximated based on data on value of travel time (VoT) from (ASEK, 2016) The calculation of VoT can be seen in appendix A.1. Like the increase in travel times, the effect on travel costs are small for single vehicles. When aggregating the effects on travel cost over time, however, the results become more evident. The passive driving style at a MPR_{AT} of 75 % generated a TTC increase of 109 SEK/km · h, which is little in regard to the high traffic flow. If one assumes that the traffic flow of 3500 veh/h is kept during 5 hours per day, and the motorway stretches 10 km through an urban area with traffic in both directions, the resulting TTC increase is approximately 4 million SEK anually. If, instead, $MPR_{AT} = 100$ % is assumed, the annual TTC increase would be approximately 7.7 million SEK.

4.1.2 CO_2 emissions

In table 4.3, the simulated emissions from all vehicles in scenario A is shown. The simulations were run five times with random seeds. The results were compared to a base simulation, in which MPR_{AT} was set to 0 %, e.g no AT:s were present. A two-sided t-test is used to determine whether the simulated results differ significantly from the base simulation. The significance level is set to 0.05. "Mix" corresponds to a vehicle distribution according to chapter 3.2. The results from all simulation runs can be found in appendix A.4.

In scenario A, the simulated amount of CO_2 emissions differed significantly from the base simulation (see table 4.3). Surprisingly, both the passive and the aggressive driving styles resulted in decreases in total amounts of emitted CO_2. All AT:s are assumed to strictly keep the speed limit, which makes the average speed of the truck fleet decrease as the AT penetration rate increases. Other aspects of the AT driving behaviour could have an impact on the amounts of emitted CO_2. Lower speed deviations ($speedDev$) and driver imperfections ($sigma$), makes the AT:s keep a smoother speed profile, with less fuel-consuming accelerations.

The passive driving style generated the largest CO_2 reductions. When simulating a passive driving style with $MPR_{AT} = 100$ %, the total CO_2 emissions decreased with 16.2 %. The aggressive driving style generally resulted in emission levels more similar to the base simulation. This behaviour is likely to be linked to the travel time increases. The passive AT:s caused the travel times to increase, which is a result of vehicles keeping lower average speeds. While the increase in travel time and travel cost is negative in the aspect of the driver, it generates positive effects on the total amounts of CO_2 emissions.

Table 4.3: Emissions from all vehicles in simulation A [kg]. Traffic flow = 3500 veh/h. "Mix" corresponds to a vehicle distribution according to chapter 3.2.

		Passive			Aggressive			Mix
Simulation	Base	50%	75%	100%	50%	75%	100%	50%
Mean	5908	5538	5218	5065	5671	5737	5593	5307
Diff [%]		-4.0%	-12.5 %	-16.2 %	-3.0 %	-5.5 %	-6.6 %	-11.9 %
p-value		<0.01	<0.01	<0.01	<0.01	<0.01	<0.01	<0.01
Reject H_0?		Yes	Yes	Yes	Yes	Yes	Yes	Yes

4.2 Results from scenario B

The results from simulations in scenario B can be seen in tables 4.4, 4.5, 4.6 and 4.7. The tables show the values of the parameter *timeLoss* and the total amount of emitted CO_2. *timeLoss* represents the average travel time increase for all vehicles in the simulation

4.2.1 Travel times

Tabls 4.4, 4.5 and 4.6 together with figures 4.1 and 4.2 show the average increases in travel times for all simulations in scenario B. When the MPR_{AT} is set to 50 %, value of the *timeLoss* parameter increases linearly with an increased traffic flow (see figure 4.1). As expected the *timeLoss* parameter get the highest values when the AT speed is 30 km/k. Since the traffic flow is far below the road capacity, the travel time increase is mostly due to the increased number of lane-changes that occur due to overtakings of the slow AT:s. When the penetration rate is 50 %, the flow of freight vehicles is a mixture of slow AT:s and regular trucks driving at higher speeds. Regular freight vehicles are therefore forced to drive in lane 2 and 3 which hinders the passenger traffic (see figure 4.3).

By investigating figure 4.2 one can see that the maximum *timeLoss* value is lower for all AT speeds when simulating a MPR_{AT} of 100 %. This is also the case for a traffic flow of 500 veh/h and 300 veh/h. The *timeLoss* value is generally lower in figure 4.2 which indicates that a flow of freight vehicles that consists of a mixture of slow AT:s and regular AT:s disturbs the traffic flow more than a flow that consists solely of AT:s.

As expected, the largest *timeLoss* value is generated when the AT:s drive at a speed of 30 km/h. The increase is however relatively small in comparison to the travel time along the entire route. A *timeLoss* value of 1.05 seconds corresponds to a travel time increase of approximately 0.3 %.

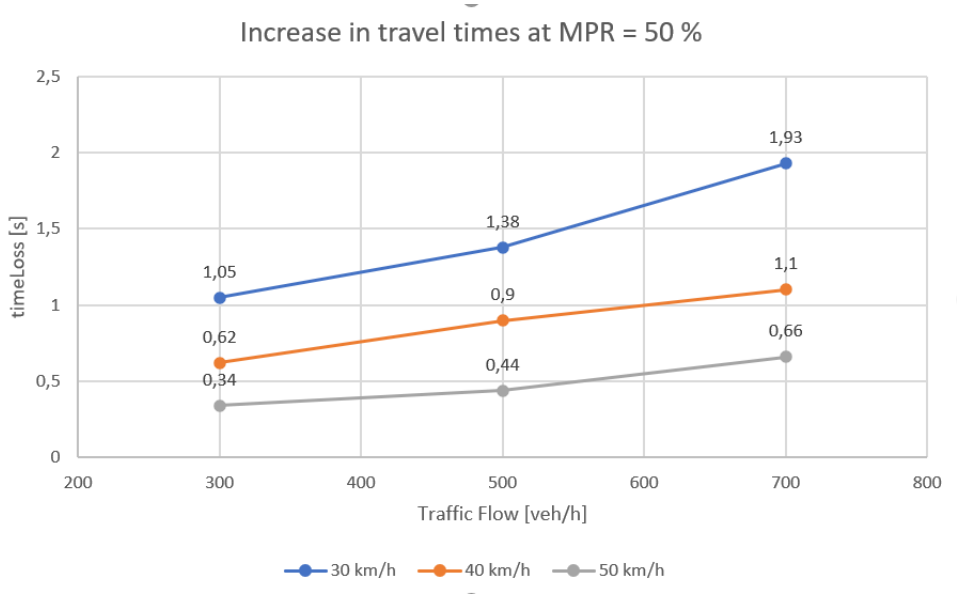

Figure 4.1: Increases in travel times in scenario B when using a MPR_{AT} of 50 % .

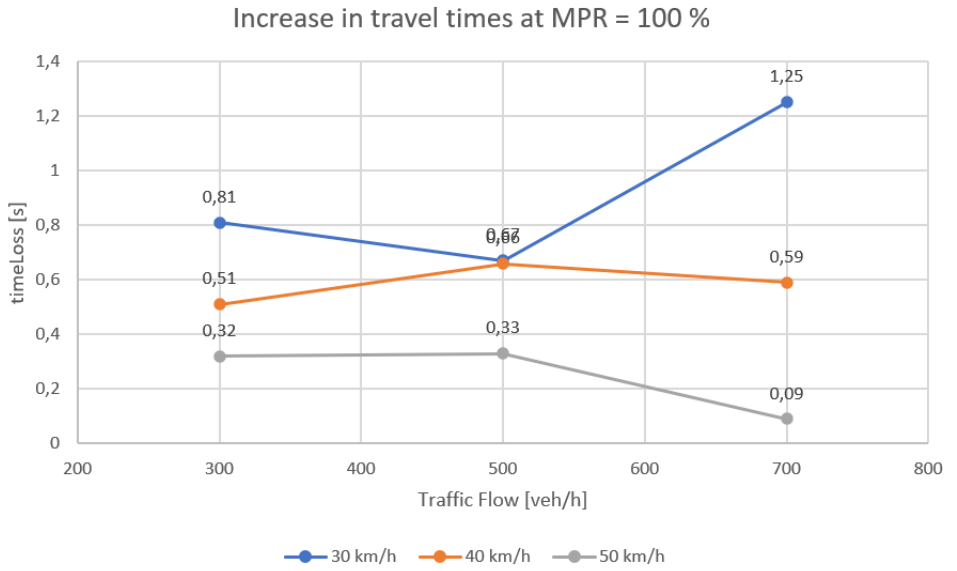

Figure 4.2: Increases in travel times in scenario B when using a MPR_{AT} of 100 % .

Table 4.4: Increase of average travel times when introducing AT vehicles at different penetration rates and speeds [s]. Traffic flow = 300 veh/h.

	Penetration rate = 50 %			Penetration rate = 100 %		
Simulation run	30 km/h	40 km/h	50 km/h	30 km/h	40 km/h	50 km/h
Mean *timeLoss* increase [s]	1.05	0.62	0.34	0.81	0.51	0.32
p-value	<0.00001	<0.00001	<0.00001	<0.00001	<0.00001	<0.00001
t-value	-14.60	-11.52	-9.81	-11.18	-13.60	-9.29
Reject H_0?	Yes	Yes	Yes	Yes	Yes	Yes

Table 4.5: Increase of average travel times when introducing AT vehicles at different penetration rates and speeds [s]. Traffic flow = 500 veh/h.

	Penetration rate = 50 %			Penetration rate = 100 %		
	30 km/h	40 km/h	50 km/h	30 km/h	40 km/h	
50 km/h						
Mean *timeLoss* increase [s]	1.38	0.90	0.44	0.67	0.66	0.33
p-value	<0.00001	<0.00001	<0.00001	<0.00001	<0.00001	<0.00001
t-value	-11.61	-26.42	-16.32	-9.98	-10.61	-11.41
Reject H_0?	Yes	Yes	Yes	Yes	Yes	Yes

Table 4.6: Increase of average travel times when introducing AT vehicles at different penetration rates and speeds [s]. Traffic flow = 700 veh/h.

	Penetration rate = 50 %			Penetration rate = 100 %		
	30 km/h	40 km/h	50 km/h	30 km/h	40 km/h	
50 km/h						
Mean *timeLoss* increase [s]	1.93	1.10	0.66	1.25	0.59	0.09
p-value	<0.00001	<0.00001	<0.00001	<0.00001	0.000023	0.21
t-value	-16.96	-14.43	-6.98	-7.48	-5.65	-1.29
Reject H_0?	Yes	Yes	Yes	Yes	Yes	No

Figure 4.3: Vehicles travelling at high speeds (yellow) overtaking slow AT trucks (red)
.

4.2.2 CO_2 emissions

Even though the increased travel times are relatively small, the effects become more evident, when investigating CO_2 emissions. Table 4.7 shows the increase of the total amount of emitted CO_2 during simulations B1 to B9. The combination of an AT speed of 30 km/h and an AT penetration rate of 50 %, that generated a travel time increase of 1.05 seconds, resulted in a significant increase in total emissions (4.7). As the traffic flow increases, the CO_2 emissions increase rapidly. At a traffic flow of 700 vehicles per hour and an AT speed of 30 km/h, the increase in CO_2 emissions per vehicle was 0.29 kg, which corresponds a relative increase of 119.8 % compared to the simulated emissions without autonomous trucks.

The rapid increase in emissions is partly due to the emissions from regular (non-autonomous) trucks. Figure 4.4 shows the registered emissions from 10 random non-autonomous trucks during one hour of simulation, with and without autonomous trucks present in the network. The figure clearly shows that when autonomous trucks are introduced in the simulations at a penetration rate of 50 % and with low speeds, the non-autonomous trucks emit larger amounts of CO_2. The data was gathered every fifth second during the 1-hour simulation. At some time instances, the emissions from some trucks were 0.0 kg/h, indicating that the trucks were coasting. The 0.0 values have been removed from the plot in figure 4.4, which means that the figure does not tell anything about the total amounts of emitted CO_2. However, it gives a clear indication on why the total average emissions per vehicle, shown in table 4.7, increased. Figure 4.4 also shows that the dispersion in registered CO_2 emissions increased when AT:s were present.

Already at a traffic flow of 300 vehicles per hour, the relative increase in CO_2 emissions is significant. When the AT:s drove at a speed of 50 km/h, approximately 30 % below the speed limit, the average increase of CO_2 emissions per vehicle was 35.4 %. Worth noticing is the relatively low speed limit on this part of motorway E6. A few simulations were run with a speed limit of 90 km/h instead of 70 km/h. The relative speed difference between an AT at 50 km/h and the resulting traffic was thus approximately 45 %. After five sequential simulation runs, the average increase in CO_2 emissions per vehicle compared to the base simulations was 61.2 %. The increase was thus not proportional to the relative increase of the speed limit, indicating that on motorway sections with a higher peed limit, the CO_2 emissions could be far greater than what the results from this scenario show.

Table 4.7: Increase of total CO_2 emissions after introducing AT:s with a speed of 30 km/h at a penetration rate of 50 %. Simulation time = 1 hour.

Flow [veh/h]		AT speed		
		30 km/h	40 km/h	50 km/h
300	Total increase [kg]	245.5	218.8	185.6
	Increase per vehicle [kg/veh-km]	0.12	0.10	0.09
	Increase per vehicle [%]	48.5 %	41.7 %	35.4 %
500	Total increase [kg]	840.8	707.8	649.3
	Increase per vehicle [kg/veh-km]	0.23	0.20	0.18
	Increase per vehicle [%]	96.2 %	81.0 %	74.3 %
700	Total increase [kg]	1466.2	1239.4	1107.9
	Increase per vehicle [kg/veh-km]	0.29	0.25	0.22
	Increase per vehicle [%]	119.8 %	101.3 %	90.5 %

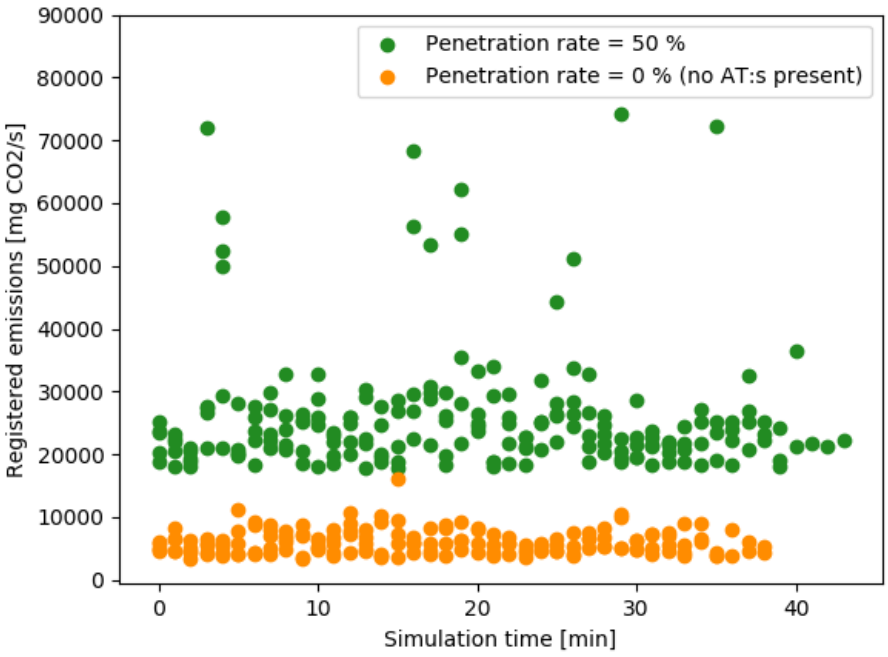

Figure 4.4: Registered emissions from regular trucks (non autonomous) before and after autonomous trucks have been introduced.

4.3 Results from scenario C

In this section, the results from scenario C are shown. Figure 4.5 shows a flow-speed diagram from the base simulation without autonomous vehicles. The simulation was run three times, each time with a random seed. As the figure shows, the flow

in lane 1 breaks down when it reaches approximately 1100 vehicles per hour. This represents the breakdown flow, in other words, the highest registered flow rate in the lane during stable conditions. When the flow rate surpasses the breakdown flow, the speed decreases rapidly, and congestion occurs in lane 1. The adjacent lanes 2 and 3 do not show any signs of flow breakdown during the simulation. Worth noticing though is that in both lane 2 and 3 the speed decreases linearly with an increasing flow rate.

Figure 4.6 shows a trajectory plot for all vehicles in the base simulation (no AT:s present). The color and the vertical axis represents the vehicle's speed. At distance = 0 meters the vehicles enter the simulation network and accelerates to their desired speeds around 70 km/h (the network speed limit). In the first 10 to 15 minutes of simulation, the vehicles keep this speed throughout the whole remaining part of the network. After approximately 15 minutes however, some vehicles start decelerating around a location 6 kilometers from the start. This is the location of the network's first on-ramp (Örgryte intersection). The decelerations increase as the simulation time passes and soon congestion starts to form. The congested string of vehicles grows and by the time the simulation ends, the traffic jam is approximately 1 kilometre long. Figure 4.5 and 4.6 will be compared to the results from simulations C1 to C7.

Table 4.8: Simulated mean speeds from the base simulation as well as simulations

	MPR	Lane 1	Lane 2	Lane 3	
Base		45.21	65.97	69.89	Simulation
Passive	50 %	41.59	64.51	68.68	C1
	75 %	40.90	64.89	69.61	C2
	100 %	40.11	65.22	68.99	C3
Aggressive	50 %	41.53	64.25	69.5	C4
	75 %	43.16	63.58	68.7	C5
	100 %	44.52	63.94	68.2	C6
Future distribution	50 %	44.77	60.58	67.49	C7

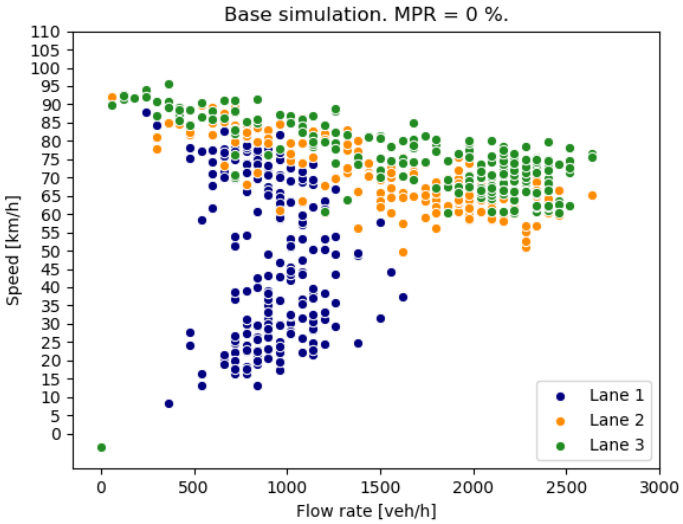

Figure 4.5: Flow-speed diagram for the base simulation without autonomous vehicles

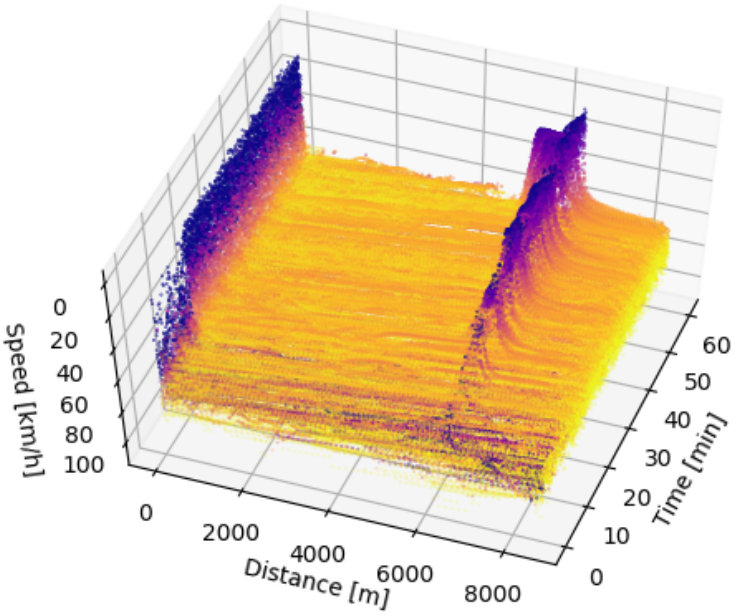

Figure 4.6: Trajectory plot for all vehicles in the base simmulation ($\text{MPR}_{AT} = 0$ %).

4.4 Simulation C1 & C4

In simulation C1 and C4, the market penetration rate of autonomous vehicles was set to 50 %. Table 4.8 shows the mean simulated speed in each lane during all simulations. The average speeds in simulation C1 and C4 are very similar. In comparison to the base simulation, the average speed in lane 1 decreases. Figures 4.7a and 4.7b, illustrates the flow breakdown in a speed-flow diagram. When simulating the conservative driving

style at a MPR_{AT} of 50 %, the flow breaks down when it reaches approximately 1000 vehicles per hour, a slight decrease compare to the results from the base simulation (see figure 4.7a). The aggressive driving style on the other hand, resulted in a flow breakdown at approximately 1100 vehicles per hour, similar to the base simulation. The adjacent lanes 2 and 3 never get congested, which results in an average speed close to the speed limit of 70 km/h (see table 4.8). It seems like the effects of the introduction of the autonomous trucks are isolated to lane 1. A reason could be that when congestion occurs in lane 1, the speed difference between lane 1 and lane 2 drastically increases. A result is that lane changing between the two lanes becomes restricted.

The differences between the conservative and the aggressive driving style are more evident when investigating the trajectory plots in figure 4.8a and 4.8b. In the simulation with conservative AT:s, the congestion in lane 1 starts to form after approximately 20 minutes and grows successively during the remaining simulation time. This means that the discharge flow (the flow out of the congestion) is smaller than the inflow, which causes a capacity drop (Yuan, V. L. Knoop and Hoogendoorn, 2014). When simulating the aggressive AT:s, the congestion does not show this behaviour. Once the congestion starts forming, the length of the string remains constant throughout the entire simulation. The congestion even disappears at some points and then reemerges (see figure 4.8b).

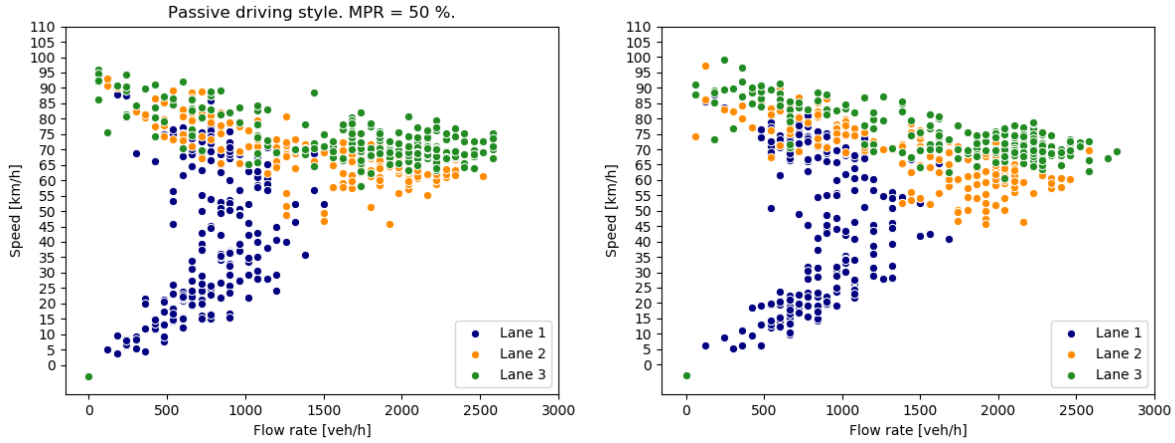

(a) Simulation C1 **(b)** Simulation C4

Figure 4.7: Flow-speed diagram for simulation C1 and C4 ($\text{MPR}_{AT} = 50$ %). "Passive driving style" corresponds to the conservative AT.

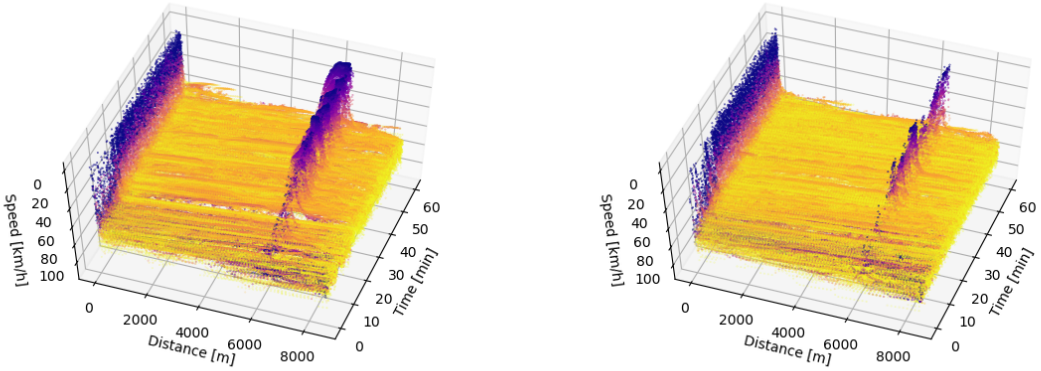

(a) Simulation C1

(b) Simulation C4

Figure 4.8: Trajectories and speeds for vehicles in simulation C1 and C4. Conservative and aggressive driving style and $\text{MPR}_{AT} = 50$ %.

4.5 Simulation C2 & C5

In scenario C2 and C5, MPR_{AT} is set to 75 %. Three quarters of the truck fleet thus consists of autonomous vehicles, whereas the remaining part is made up by regular trucks. Simulation C2 shows similar results to simulation C1 in figure 4.7a. However, when investigating figure 4.7b, lane 1 shows a higher concentration of low speeds, compared to the results with $\text{MPR}_{AT} = 50$ % in figure 4.7a. The breakdown flow in lane 1 in simulation C2 is approximately 1000 vehicles per hour, which is similar to the base simulation.

In simulation C5, the breakdown flow seems to occur around 1250 vehicles per hour, which is a slight improvement compared to simulation C4 ($\text{MPR}_{AT} = 50$ %). The situation in lane 2, however, seems to worsen a bit. Figure 4.9b shows a concentration of average speeds around 50 km/h, when the flow rate reaches approximately 2000 vehicles per hour. In table 4.8, one can see that the average speed in lane 2 slightly decreases compared to both simulation C2 and the base simulation. One reason could be that the aggressive AT:s are more likely to perform lane changes. When the speed in lane 1 drops, the AT:s are likely to change lane in order to keep their desired speeds, which affects the flow in lane 2. The flow in lane 3 is not affected significantly during the simulation, resulting in an average speed close to the speed limit (see table 4.8).

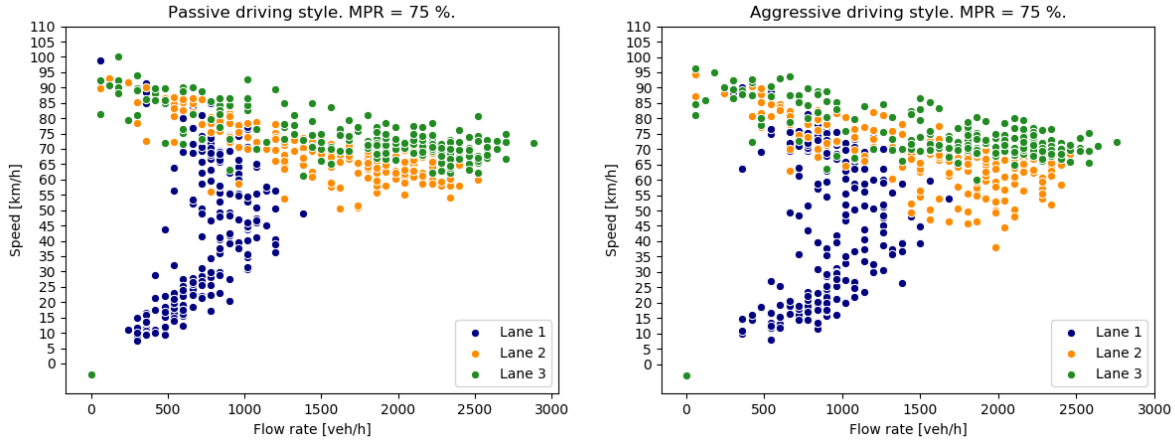

(a) Simulation C2 **(b)** Simulation C5

Figure 4.9: Flow-speed diagram for simulation C2 and C5 ($\text{MPR}_{AT} = 75$ %). "Passive driving style" corresponds to the conservative AT.

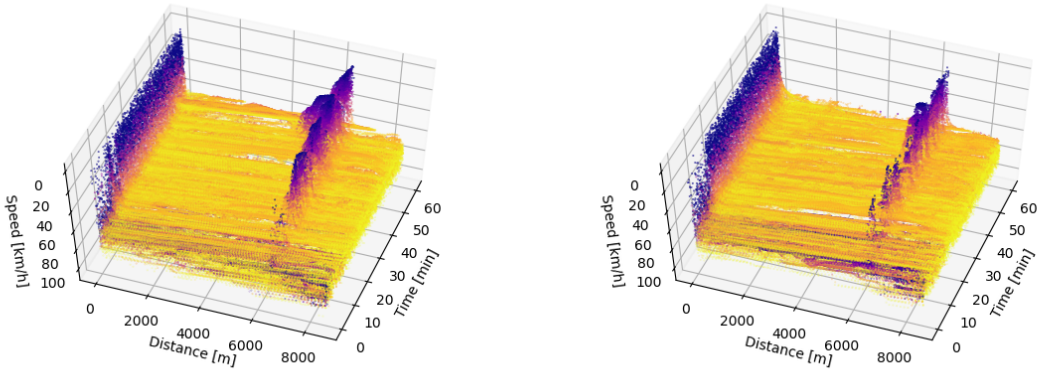

(a) Simulation C2 **(b)** Simulation C5

Figure 4.10: Trajectories and speeds for vehicles in simulation C2 and C5. Conservative and aggressive driving style and $\text{MPR}_{AT} = 75$ %.

4.6 Simulation C3 & C6

In simulation C3 and C6 an AT market penetration rate of 100 % was used. Figure 4.9a and 4.11a show the simulated flows and speeds in each lane on an aggregate level. When looking at the conservative driving style, congestion in lane 1 occurs at a traffic flow of approximately 1000 vehicles per hour, similar to the results from simulation C2 (see figure 4.9a and 4.11a). In lane 2 and 3, the speed decreases linearly as the flow rate increases. Unlike lane 1, there are no signs of sudden drops in speeds during the simulation.

Figure 4.12a shows the trajectory plot in for simulation C3. Congestion starts forming after approximately 10 minutes. At first, the length of the traffic jam does not increase

substantially. However, after approximately 30 minutes of simulation, the flow suddenly breaks down, creating a congestion shock wave downstream in lane 1. The string of congested vehicles grows and at the end of the simulation the length of the traffic jam is approximately 2 kilometers, which is significantly longer than in simulation C2. In the road section prior to the on-ramp at 6000 meters, the speed homogeneity and the average speed seems to have increased compared to all other simulations with the conservative AT:s and to the base simulation (see figure 4.12a). The conservative AT:s keep to the rightmost lane, which makes the faster cars use lane 2 and 3. As faster vehicles are not hindered by the AT:s, they can keep their desired speeds. In table 4.8, one can see that the average speed in lane 2 increases with an increasing market penetration rate of conservative AT:s.

The results from simulation C6 indicate a breakdown flow in lane 1 at approximately 1250 vehicles per hour, like simulation C5 (see figure 4.11b). The average speed in lane 1 increased from 43.1 seconds in simulation C5 to 44.52 in simulation C6 (see table 4.8). In lane 2 and 3, the results are similar to simulation C5. At a flow rate of approximately 1500 to 2000 vehicles per hour, the speed slightly drops and there is a large variation in registered speeds. As stated in section 4.5, this is assumed to be caused by the aggressive AT:s' lane changing behaviour.

Figure 4.12b shows the trajectories in simulation C6. Compared to simulation C5, it takes longer before the speed in lane 1 drops. After approximately 30 minutes, a short string of vehicles slows down creating a source of congestion. Unlike simulation C5, the outflow from the congestion source is kept similar to the inflow, making the length of the congestion remain constant during the resulting simulation time. At high penetration rates, the conservative driving style seems to have worse effect on capacity than the aggressive driving style, given the presence of on-ramps with significant traffic flows.

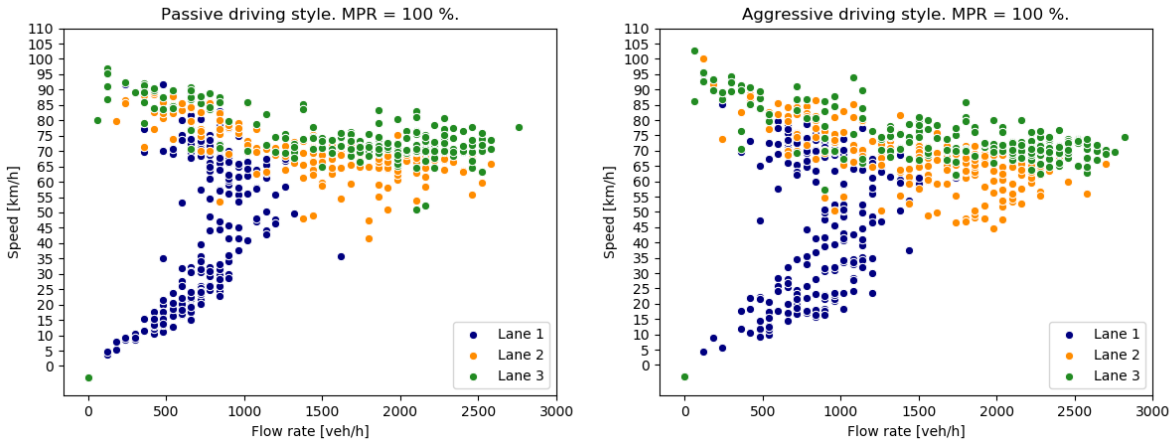

(a) Simulation C3. **(b)** Simulation C6.

Figure 4.11: Flow-speed diagram for simulation C5 and C6 (MPR_{AT} = 100 %). "Passive driving style" corresponds to the conservative AT.

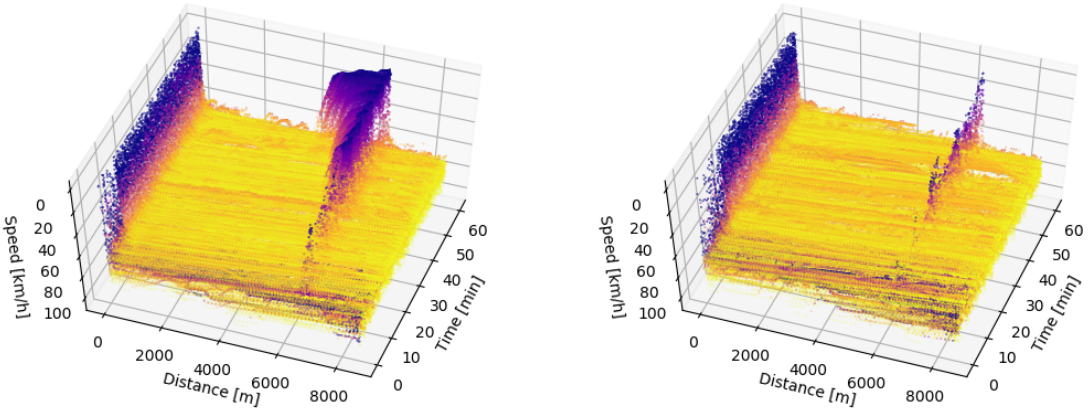

(a) Trajectories for vehicles in simulation C3.

(b) Trajectories for vehicles in simulation C6.

Figure 4.12: Trajectories and speeds for vehicles in simulation C5 and C6. Conservative and aggressive driving style and $\text{MPR}_{AT} = 100$ %.

4.7 Simulation C7

In simulation C7, the vehicle distribution according to section 3.1 was simulated. Figure 4.13 shows the flow-speed diagram, in which the breakdown flow in lane 1 can be seen. Similar to the base simulation, the speed and flow in lane 1 drops at a flow rate of approximately 1100 vehicles per hour. The trajectory plot in figure 4.14 however, shows that the flow breakdown in the base simulation was more severe than in simulation C7. In contrast to the base simulation, the length of the string of congested vehicles in simulation C7 is similar throughout the whole simulation (see figure 4.14). This indicates that the discharge flow, e.g the flow out of the congestion, is higher in simulation C7 compared to the base simulation.

In the trajectory plot, the speed before the congested road section seems to be more homogeneous in comparison to the base simulation. By looking at figure 4.6 one can observe an orange colour for the traffic before the congested road section, which indicates that some vehicles are driving with a lower speed than in figure 4.14. The trajectories of the slower vehicles are plotted on top of the trajectories of faster vehicles, which makes it impossible to get any information about the average speed from figure 4.6. However, it indicates that the base simulation has a larger speed heterogeneity. The AT:s have a *speedDev* parameter equal to 0, which means that they do not deviate from the speed limit. A MPR_{AT} of 50 % seems to greatly increase the speed homogeneity in the traffic flow.

According to table 4.8, the average speed in simulation C7 is lower than in the base simulation. This is likely due to the significant share of vehicles (AT:s) which do not deviate from the speed limit and thus reduce the average speed.

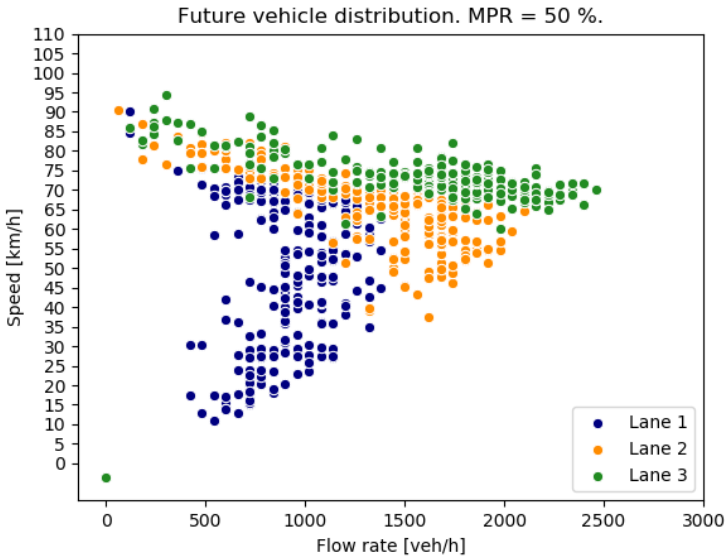

Figure 4.13: Flow-speed diagram for simulation C7.

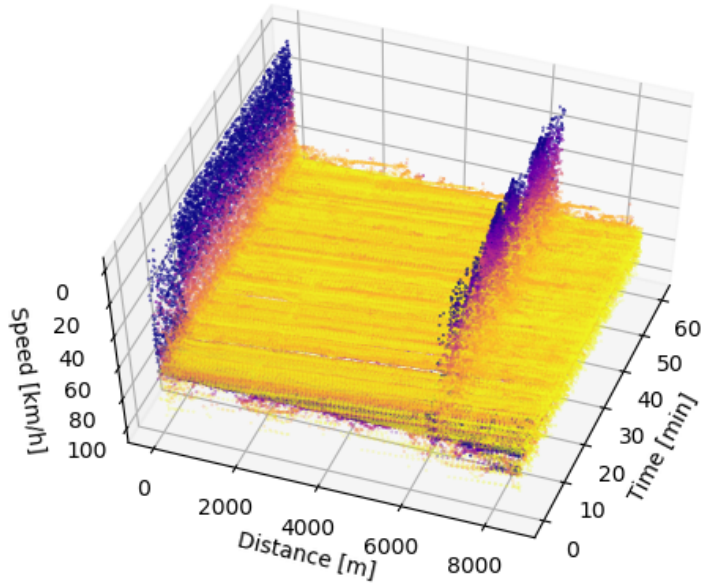

Figure 4.14: Trajectory diagram for simulation C7, showing each vehicle's speed along its route.

5 Analysis and discussion

The three scenarios A, B and C have showed that autonomous trucks indeed have an impact on both traffic flow characteristics as well as emissions of CO_2. In this section the results will be analysed in relation to the research questions in section 1.3.

5.1 Traffic flow

In scenario A, the effect on traffic flow and emissions were investigated at high, but stable, traffic flows. The conservative driving style turned out to affect the traffic flow the most, generating travel time increases ranging from 0.87 % to 2.53 %. When the penetration rate of conservative AT:s increased, the average travel time increased which indicates that the conservative driving style disturbs the regular traffic flow. One explanation for this behaviour could be that the speed deviation of the AT:s are smaller than that of the regular trucks. The AT:s are in other words more likely to respect the speed limitations. The regular trucks and cars, however, have desired speeds that are larger than the speed limit, which means that the AT speed deviates from the average speed on the route. With an increasing AT penetration rate, the speed differences between AT:s and the surrounding traffic are therefore likely to increase, which in turn make the cars need to perform time- and fuel consuming overtaking maneuvers. When vehicles change lane from lane 1 to lane 2, vehicles in lane 2 need to adjust their speed to facilitate the overtaking procedure. The travel time does therefore not only increase for vehicles performing the lane changes, but also for vehicles in the adjacent lanes.

The conservative AT:s also showed to affect the total road capacity negatively. In scenario C, the conservative AT driving style caused the capacity in lane 1 to drop, in comparison to the base simulation. The conservative AT driving style represents an AT in early stages of AT development, as mentioned in section 3.2. When AT:s are introduced on motorways for the first time, it is therefore likely that one can expect a slight drop in road capacity and increases in travel times. Once the driving characteristics of the AT:s improve and lane-changing maneuvers can be performed like any other truck, the AT driving characteristics will be more similar to that of the aggressive AT. The results indicate that an increasing rate of aggressive AT:s will instead improve the traffic flow. The truck fleet is however, not likely to consist solely of conservative or aggressive AT:s, but rather of a mixture of them both. Once AT:s with a more advanced driver behaviour is introduced, the conservative AT:s are likely to be deprecated. Based on the results from this thesis it is not possible to determine how the traffic flow will be affected by this type of combination of conservative and aggressive AT:s. It is likely however, that once "aggressive" AT:s are introduced, the negative impacts of the conservative driving style will be reduced. Even further on in development, V2V communication systems will emerge, which enable connected

autonomous vehicles to communicate with each other (Calvert, Schakel and Lint, 2017).

A potential future vehicle distribution, containing both connective cars and AT:s with V2V technology was simulated in scenario A and C. The market penetration rate of autonomous vehicles was set to 50 %, which means that the vehicle flow consisted of 50 % manual vehicles and 50 % vehicles with some level of autonomy. Scenario A showed, that when there is a mixture of autonomous and manual vehicles, the travel times trough a network with dense traffic could increase due to the speed difference between the autonomous and the manual vehicles. The travel time increase is measured with the *timeLoss* parameter, which calculates the difference between a vehicle's actual and desired travel time (German Aerospace Center, 2019a). The AT:s will have a longer desired travel time than the regular trucks and if no larger disturbance occurs along the route, the actual travel time will equal the desired travel time, resulting in *timeloss* close to zero. The travel time of the regular vehicles however, will be increased due to interactions with the slower AT:s, resulting in larger *timeLoss* values. The travel time increases in the "future" vehicle distribution, is therefore mostly a result of travel time reductions among the non-autonomous vehicles. When the share of autonomous vehicles become significantly higher and the homogeneity in the traffic flow increases, the effect on the *timeloss* parameter is therefore likely to decrease.

The effect on travel times were small in scenario B. Chapter 4.2 showed that the total travel time increase was less than 1 %. At very low traffic flows there is free capacity in lane 2 and 3 which enables fast overtakings. However, if the traffic flow were to significantly, this might not be the case. The effects on travel time could therefore become much larger if the nighttime AT traffic continued into the morning hours, when the traffic flow rapidly increases.

When investigating the effects of autonomous vehicles it is important to bear in mind that the time horizon of the deployment of autonomous vehicles on Swedish roads is uncertain. When simulating the passive and aggressive AT:s in this thesis, a traffic environment without autonomous cars has been simulated. Depending on when AT:s are to be allowed on public roads, the AV technology could be more or less progressed. If the deployment of the first AT:s will happen in a distant future, the autonomous technologies could be far more advanced than what has been modelled in this thesis and V2V technology could be standard equipment in any AT. Alternatively, connectivity, such as V2V communication systems, could become prerequisites for the AT:s to be allowed on Swedish roads. In such cases, not the passive nor the aggressive AT, simulated in this thesis, will be present in the traffic flow. Most likely, however, is that the AT deployment will be gradual, with lower levels of AT:s in initial stages and connected AT:s later in development. In Jönköping, Sweden, a fully automated truck is in use on public roads between two freight terminals Einride (2019). The route is short, and the truck needs to be monitored externally by a human being in order to be allowed in traffic. The truck is not near any fully automated vehicle simulated in this report. However, it indicates that permissions to drive AT:s could come soon enough for non-connected AT:s to be present in the traffic flow.

5.2 Traffic cost

In scenario A in chapter 3.2.1, the increase in traffic cost (cost experienced by drivers whose travel time increases) was 7.7 million SEK annually when simulating a MPR_{AT} of 100 %. In relation to the large number of vehicles that pass through the investigated section of motorway E6 during a year, a total travel cost increase of 7.7 million SEK is rather small. Important to note however, is that during the simulations in scenario A, the traffic flow was kept stable during all simulations. As argued in chapter 1.5, due to the limited network size modelled in this thesis, it is impossible to analyse when congestion would occur in reality at the geographical location in Gothenburg. A more severe bottleneck further ahead (beyond our simulated network) could cause congestion earlier than what has been shown in simulations. In fact, the loop detector data from Trafikverket (2019) indicates that congestion regularly occurs during peak hours when the traffic flows are similar to those in scenario A. By introducing conservative AT:s that disturb the traffic flow, the risk of more severe congestion increases. This would generate much larger increases to the travel costs, than the 7.7 million SEK that was simulated in scenario A.

5.3 Environmental aspects

In all simulations it is assumed that all AT:s use diesel and passenger cars use gasoline. All simulated vehicles thus emit CO_2. In the future use of AT vehicles, there is a possibility however, that a significant share of AT:s will be electric. Kristoffersson and Brenden (2018) describe a future scenario of autonomous freight, in which kilometer-charging systems on vehicles running on fossil fuels and bans on such vehicles in city centres, have forced the truck fleet to go green. Hatch and Helveston (2018) argues that there are several reasons why autonomous vehicles will be electric. Electric vehicles will need less maintenance, be cheaper to fuel and recharging could easily be monitored by the vehicle itself, which is not the case for the regular vehicles. This development is however not for certain. Hatch and Helveston (2018) further mention examples of transport service companies which have revealed that their future AV:s will run on fossil fuels. Due to the uncertain future of AV electrification, the autonomous vehicles in these simulations have been kept non-electric.

Scenario B showed that introducing slow AT:s at night has an effect on overall emissions of CO_2. The slow AT:s used the rightmost lane, which forced the surrounding traffic to constantly perform energy consuming lane-changing procedures. When the regular trucks occupied lane 2, cars had to use lane 3 in order to overtake the trucks. As mentioned above, all trucks use diesel as fuel whereas the passenger vehicles are gasoline cars. Any increase in energy consumption thus directly affect the total CO_2 emissions. From an environmental perspective, a perquisite for introducing slow AT:s at night should therefore be that a significant share of either the truck fleet or the passenger vehicle fleet is electrified. As argued by Hatch and Helveston (2018), this is likely to be the case. Given that electricity is generated from renewable sources, the potential energy increase related to nighttime AT traffic, would in such a case not cause increases to total emissions of CO_2.

Scenario B further showed that the amount of emitted CO_2 per vehicle increased significantly when the flow rate increased. If slow AT:s with very low speeds such as 30 km/h are introduced, it is important to restrict the traffic to times when the traffic flow is very low. In the case of motorway E6, the flow rate reaches below 200 veh/h at the lowest, but in the early morning hours, the traffic flow quickly increases. In order to ensure a low traffic flow, so that CO_2 emissions are kept at a low level, nighttime AT traffic should only occur within strict time intervals. Like scenario A, the increase in CO_2 emissions was simulated based on the assumption that the vehicle fleet is running 100 % fossile fuels. If a share of the vehicle fleet is electrified, as in predictions by Hatch and Helveston (2018) and Kristoffersson and Brenden (2018), more generous time intervals could be accepted. Scenario B showed that negative effects on travel times were very limited even at traffic flows up to 700 veh/h. The main issue with the nighttime AT traffic is thus the CO_2 emissions.

5.4 Merging behaviour in junctions

The focus in this thesis has been AT:s with lower automation levels. In the "future" vehicle distribution however, AT:s and cars equipped with CACC technologies were simulated. As figure 3.1 shows, cooperative trucks made up only 3.4 % of the total traffic flow in the future vehicle distribution. At low shares of connected AV:s, the occurrence of vehicle platoons will be relatively limited. In heterogeneous flows of several vehicle types, it will take time for such vehicles to form platoons. Due to the relatively short travel time through the network, truck platoons were rare. Modelling a larger network would likely increase the likelihood of platoons forming inside the network, and thus increase the realism in the simulations. However, due to the scope of this thesis, the network size has been kept relatively short.

If the share of connected AT:s was to significantly increase in reality, truck platoons would most likely be common on motorways. This could cause problems at on- and off-ramps. Figure 5.1 shows a platoon of five connected AT:s in a platoon passing an on ramp, on which a passenger car accelerates and tries to enter the motorway. However, this manoeuvre is hindered by the long platoon occupying lane 1, which forces the car to break. The platoon can split in order to facilitate for instance a lane change, however, the time it takes for a vehicle platoon to split and make room for an incoming vehicle is too long and results in insufficient merging procedures. Analogously, similar problems could occur also at off-ramps. Depending on the strategic lane changing behaviour, some vehicles might change from lane 2 to lane 1 right before continuing onto the off-ramp. If a long truck platoon was to hinder this lane changing behaviour by occupying lane 1, it could result in sudden and urgent breaking manoeuvres. In the simulated "future" vehicle distribution this happens very rarely, but due to the uncertainty in the deployment of AT:s, it is an important aspect to keep in mind.

Figure 5.1: A platoon of connected AT:s hindering an incoming car on an on-ramp to enter lane 1.

6 Conclusions

This thesis has showed that autonomous trucks are likely to affect both traffic flows, travel times and emissions of CO_2, once they are introduced in the Swedish road network. At first, the driver behaviour of AT:s will be conservative in comparison to that of regular trucks. When simulating this type of AT driver behaviour, the results indicates losses in maximum road capacity and increases to average travel times and travel costs. In the first phases of automation of the truck fleet, it is therefore likely that positive aspects of AT:s, such as economical savings and increased traffic safety, are partly compensated by other negative traffic flow related effects. It is therefore vital to ensure that the early stages of deployment of AT:s comes with sufficient time restrictions, in order to avoid loss of capacity in e.g rush hours close to busy urban centers.

Once AT:s with enhanced lane-changing capabilities become commercially available, negative effects on road capacity, travel times and travel costs are expected to decrease. When simulating a traffic flow consisting of regular cars, trucks and AT:s with better lane changing capabilities, the maximum road capacity increased, compared to base simulations without AT:s. Furthermore, the effect on travel times was insignificant, proving that AT:s with a more "aggressive" driving style in contrast to the conservative ones, perform better and do not disturb the traffic flow. It is therefore likely that when AT:s with conservative driving styles are successively phased out and replaced with AT:s with higher levels of automation, the effects on road capacity will improve.

As stated by Kristoffersson and Brenden (2018), removing the truck driver and replacing it with autonomous driving technology enables trucks to operate during nighttime to a larger extent than today. Furthermore, in order to save energy, the truck traffic at night could keep a much lower speed than usual. When simulating an increased truck share at night, including AT:s with low speeds, travel times were moderately affected. The results showed however, that the total emissions of CO_2 increased significantly. When the traffic flow increased from 300 to 500 vehicles per hour, the average CO_2 emissions per vehicle doubled. When introducing nighttime AT traffic, it is therefore crucial to restrict it time-wise and geographically in order to ensure that the nighttime AT:s always operate in low traffic flows. In this work all vehicles are assumed to run on fossil fuels. Like Hatch and Helveston (2018) mentions however, it is likely that a share of future AT:s will be electric. If this is were to be the case, negative environmental effects could possibly be compensated.

6.1 Further research

As mentioned in chapter 1.5, the network size used in this work is small. In total, the simulated motorway is 8.6 km long and contains two grade separated intersections. An effect of the relatively short motorway section, is that very few platoons have time to

form within the network. In order to extend this research, a future vehicle distribution made up by both higher and lower levels of AV:s and regular vehicles could be simulated in a larger motorway network. By doing so, the effects of vehicle platoons could be captured in a more realistic way. Furthermore, a larger network would enable analysis of effects on traffic flow when the characteristics of the motorway change. For instance, the speed limitations could vary throughout the network, as well as the design of the grade separated intersections.

As this work has exclusively focused on an urban motorway setting, including other types of infrastructure in the network could be a way to extend this research. As discussed in chapter 1.5, by limiting the network to only a motorway and its on- and off-ramps, many aspects of autonomous truck traffic is excluded. Even though a large share of the total route length might be located on motorways, AT:s will need to navigate through e.g. signalised intersections, roundabouts, and other types of infrastructure in order to get to the motorway. Tolerable effects in such settings could thus be a perquisite for deploying AT:s on motorways and would therefore be an interesting topic for further research.

Another way to extend this research would be to include electrical vehicles (EV:s) in order to resemble the future vehicle fleet in a more detailed way. As mentioned in chapter 5.3, Hatch and Helveston (2018) argued that it is likely that the introduction of autonomy within the vehicle sector would come with some degree of electrification. To model such a scenario, the emission levels could be changed when defining the simulated vehicle types. In this way, other vehicle types such as hybrid cars could be modelled.

Appendices

A Appendix

A.1 Calculation of Value of Time (VoT)

The calculation of Value of Time is based on data from ASEK (2016). It defines four categories of trips, as shown in table A.1. In scenario A, a flow of approximately 3500 vehicles per hour was simulated, which corresponds to the traffic flow in the early morning peak. At this time, the share of cars was 83 %. Since no information about trip purposes was available for the particular stretch of motorway in Gothenburg, the share of work trips is an approximation. It is assumed that 60 % of the car traffic is made up of work-trips. This corresponds to 50 % of the total traffic flow. Analogously, the resulting 40 % of the car traffic is assumed to be made up of trips with other purposes than commuting. This share corresponds to 33 % of the total traffic flow (see table A.1). The share of freight vehicles is approximated from the vehicle types in the simulations.

ASEK (2016) provides VoT-values for 2014 and at 2040. The VoT values shown in table A.1 are thus approximated with linear interpolation. It is assumed that on average, 1.5 people travel in each car. Therefore, the VoT related to cars is multiplied with 1.5.

Table A.1: Approximations of the value of time (VoT). Data from: ASEK (2016).

Trip category	**Share [%]**	**VoT (2035) [SEK]**	**Total [SEK]**
Car Work	50	129	64.0
Car Other	33	87	29.0
Σ			*93.0*
$\Sigma \cdot 1.5$			*139.5*
Freight no trailer	10	9	1.0
Freight trailer	7	45	3.1
Σ			*4.1*
Weighted VoT [SEK]			143.6

A.2 Levels of autonomous vehicle technology

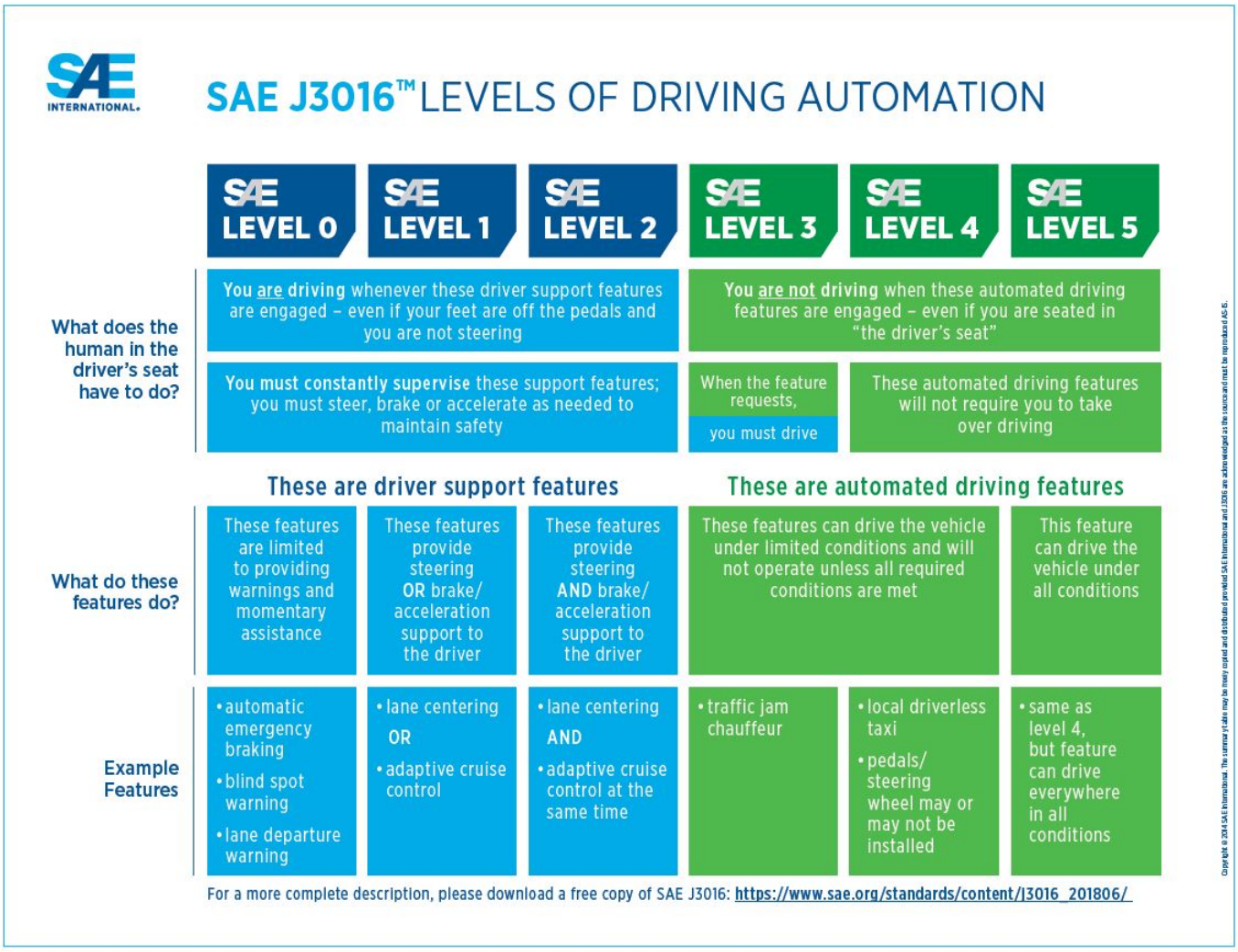

Figure A.1: Levels of autonomous vehicle technology defined by SAE International. Source: SAE (2019)

.

A.3 Simulated increase in travel times in scenario B. 10 random seeds for each combination of AT speed and traffic flow.

Table A.2: Increase of average travel times when introducing AT vehicles at different penetration rates and speeds [s]. Traffic flow = 300 veh/h.

	Penetration rate = 50 %			Penetration rate = 100 %		
Simulation run	30 km/h	40 km/h	50 km/h	30 km/h	40 km/h	50 km/h
1	0.91	0.56	0.29	0.60	0.40	0.38
2	0.99	0.53	0.27	1.11	0.56	0.32
3	1.02	0.54	0.27	0.75	0.40	0.45
4	0.71	0.50	0.24	0.96	0.79	0.36
5	1.38	0.76	0.38	0.89	0.49	0.12
6	1.23	0.40	0.39	1.02	0.55	0.41
7	1.03	0.74	0.25	0.43	0.44	0.19
8	1.25	0.48	0.56	0.95	0.53	0.39
9	1.26	0.73	0.46	0.53	0.55	0.32
10	0.74	0.94	0.29	0.81	0.43	0.26
Mean *timeLoss* increase [s]	1.05	0.62	0.34	0.81	0.51	0.32
p-value	<0.00001	<0.00001	<0.00001	<0.00001	<0.00001	<0.00001
t-value	-14.60	-11.52	-9.81	-11.18	-13.60	-9.29
Reject H_0?	Yes	Yes	Yes	Yes	Yes	Yes

Table A.3: Increase of average travel times when introducing AT vehicles at different penetration rates and speeds [s]. Traffic flow = 500 veh/h.

	Penetration rate = 50 %			Penetration rate = 100 %		
Simulation run	30 km/h	40 km/h	50 km/h	30 km/h	40 km/h	50 km/h
1	0.98	0.74	0.35	0.51	0.50	0.45
2	1.69	0.81	0.48	0.85	0.66	0.35
3	1.09	0.91	0.56	1.07	1.02	0.18
4	1.42	0.99	0.43	0.54	0.60	0.34
5	1.18	0.87	0.44	0.62	0.79	0.45
6	1.72	0.91	0.41	0.38	0.81	0.38
7	1.32	0.84	0.38	0.87	0.42	0.32
8	1.17	1.07	0.34	0.53	0.55	0.28
9	2.16	0.82	0.53	0.67	0.46	0.26
10	1.07	0.99	0.45	0.62	0.83	0.33
Mean *timeLoss* increase [s]	1.38	0.90	0.44	0.67	0.66	0.33
p-value	<0.00001	<0.00001	<0.00001	<0.00001	<0.00001	<0.00001
t-value	-11.61	-26.42	-16.32	-9.98	-10.61	-11.41
Reject H_0?	Yes	Yes	Yes	Yes	Yes	Yes

Table A.4: Increase of average travel times when introducing AT vehicles at different penetration rates and speeds [s]. Traffic flow = 700 veh/h.

	Penetration rate = 50 %			Penetration rate = 100 %		
Simulation run	30 km/h	40 km/h	50 km/h	30 km/h	40 km/h	50 km/h
1	2.21	1.20	0.67	1.43	0.38	0.21
2	1.78	0.97	0.47	1.80	0.33	0.08
3	2.52	1.23	0.88	1.20	0.60	-0.02
4	1.41	1.04	0.57	0.93	0.50	0.22
5	2.05	0.90	1.07	0.60	0.40	0.11
6	1.68	1.35	0.39	1.50	0.41	0.04
7	1.77	0.93	0.56	2.18	0.47	0.30
8	1.86	1.11	0.54	0.97	0.68	-0.11
9	1.93	1.02	0.47	1.14	1.12	0.04
10	2.07	1.27	0.99	0.70	0.99	0.04
Mean *timeLoss* increase [s]	1.93	1.10	0.66	1.25	0.59	0.09
p-value	<0.00001	<0.00001	<0.00001	<0.00001	0.000023	0.21
t-value	-16.96	-14.43	-6.98	-7.48	-5.65	-1.29
Reject H_0?	Yes	Yes	Yes	Yes	Yes	No

A.4 Simulation results from scenario A.

In table A.5, the simulated values of the *timeLoss* parameter, e.g the simulated increases in travel time are shown. Table A.6 shows the simulated time for vehicles to enter the motorway on the on-ramp in Örgryte intersection. Lastly table A.7 shows the simulated total emissions from all vehicles in scenario A. All simulations were run 5 times with random seeds.

Table A.5: Increase of average travel times when introducing AT vehicles at different penetration rates and AT drivin styles [s]. Traffic flow = 3500 veh/h. "Mix" corresponds to a vehicle distribution according to chapter 3.2.

		AT_{pass}			AT_{agg}			Mix
Simulation	Base	50 %	75 %	100 %	50 %	75 %	100 %	50 %
1	6.59	10.11	9.41	13.30	9.30	10.44	7.72	15.08
2	8.30	10.50	8.77	14.08	8.86	10.55	8.83	14.79
3	9.02	9.27	13.02	11.48	7.58	7.90	7.63	13.85
4	8.90	8.08	10.93	13.38	6.13	7.87	8.46	15.85
5	7.39	10.79	11.03	12.76	9.38	7.65	9.65	14.28
Mean TT increase [s]		1.71	2.59	4.96	0.21	0.84	0.42	6.73
Reject H_0?		Yes	Yes	Yes	Yes	Yes	No	Yes
p-value		0.03	0.02	< 0.01	0.79	0.33	< 0.01	< 0.01

Table A.6: Increase of on-ramp merging times at Örgryte intersection, when introducing AT vehicles at different penetration rates and AT driving styles [s]. Traffic flow = 3500 veh/h. "Mix" corresponds to a vehicle distribution according to chapter 3.2.

		AT_{pass}			AT_{agg}			Mix
Simulation	Base	50 %	75 %	100 %	50 %	75 %	100 %	50 %
1	3.04	3.0	3.85	5.65	2.55	2.71	2.42	3.35
2	2.88	2.87	3.11	4.22	2.31	2.71	2.14	3.46
3	2.87	2.64	3.26	4.38	2.73	2.47	2.37	2.97
4	2.92	3.84	3.12	3.70	2.36	2.40	2.24	3.08
5	2.73	3.95	3.23	4.50	2.58	2.52	2.2	3.10
Mean TT increase [s]		0.37	0.43	1.60	-0.38	-0.33	-0.65	0.30
p-value		0.21	0.02	<0.01	<0.01	<0.01	<0.01	0.02
Reject H_0?		No	Yes	Yes	Yes	Yes	Yes	Yes

Table A.7: Emissions from all vehicles in simulation A [kg]. Traffic flow = 3500 veh/h. "Mix" corresponds to a vehicle distribution according to chapter 3.2.

		Passive			Aggressive			Mix
Simulation	Base	50%	75%	100%	50%	75%	100%	50%
1	6039	5694	5762	5755	5691	5303	5101	5186
2	5795	5739	5719	5535	5629	5101	4998	5314
3	5916	5625	5809	5489	5460	5295	4980	5311
4	5832	5597	5715	5535	5407	5197	5110	5266
5	5959	5700	5681	5650	5501	5195	5135	5456
Mean	5908	5671	5737	5593	5538	5218	5065	5307
Diff [%]		-4.0%	-3.0 %	-5.5 %	-6.6 %	-12.5 %	-16.2 %	-11.9 %
p-value		<0.01	<0.01	<0.01	<0.01	<0.01	<0.01	<0.01
Reject H_0?		Yes	Yes	Yes	Yes	Yes	Yes	Yes

Bibliography

Alipour-Fanid, Amir et al. (2017). 'String stability analysis of cooperative adaptive cruise control under jamming attacks'. In: *Proceedings of IEEE International Symposium on High Assurance Systems Engineering* December, pp. 157–162. ISSN: 15302059. DOI: 10.1109/HASE.2017.39.

ASEK (2016). 'Analysmetod och samhällsekonomiska kalkylvärden för transportsektorn : ASEK 6 . 0 Kapitel 5 Kalkylprinciper och generella kalkylvärden'. In: 6, pp. 1–45.

Bjärkvik, Erik et al. (2017). 'Simulation and Characterisation of Traffic on Drive Me Route around Gothenburg using SUMO'. In: *SUMO User Conference 2017 - Towards Simulation for Autonomous Mobility* July. URL: http://www.dlr.de/fs/Portaldata/16/Resources/projekte/sumo/Proceedings_SUMO2017.pdf.

Calvert, S. C., W. J. Schakel and J. W.C. van Lint (2017). 'Will automated vehicles negatively impact traffic flow?' In: *Journal of Advanced Transportation* 2017. ISSN: 20423195. DOI: 10.1155/2017/3082781.

E6 Highway Project (2020). URL: https://www.roadtraffic-technology.com/projects/e6-highway-project/.

Einride (2019). *World premiere: First cab-less and autonomous, fully electric truck in commercial operations on public road.* URL: https://www.einride.tech/news/world-premiere-first-cab-less-and-autonomous-fully-electric-truck-in-commercial-operations-on-public-road.

Erdmann, Jakob (2015). '1 Lane-Changing Model in SUMO'. In: January.

German Aerospace Center (2019a). *Definition of Vehicles, Vehicle Types, and Routes.* URL: https://sumo.dlr.de/docs/Definition_of_Vehicles,_Vehicle_Types,_and_Routes.html.

– (2019b). *Simulation/Output/Multi-Entry-Exit Detectors (E3).* URL: https://sumo.dlr.de/docs/Simulation/Output/Multi-Entry-Exit_Detectors_(E3).html.

– (2019c). *Sumo At a Glance.* URL: https://sumo.dlr.de/userdoc/Sumo_at_a_Glance.html.

– (2019d). *Vehicle Type Parameter Defaults.* URL: https://sumo.dlr.de/docs/Vehicle_Type_Parameter_Defaults.html.

Ginsburg, Robert and Arin Rubaci Uygur (2017). 'Changing Technology in Transportation : Automated Vehicles in Freight Authors : College of Urban Planning and Public Affairs University of Illinois at Chicago Final Draft'. In: pp. 1–27.

Gordon, Ben et al. (2018). 'The future of autonomous vehicles: Lessons from the literature on technology adoption'. In: 0003.4, p. 17. DOI: 10.1093/aepp/ppz005. URL: http://www.dot.ca.gov/hq/research/researchreports/reports/2018/CA17-2796-3_FinalReport.pdf.

Greenberg, I (1966). 'The log-normal distribution of headways'. In: *Australian Road Research* 2.7, pp. 14–18.

Grumert, Ellen F (2018). 'Using Connected Vehicles in Variable Speed Limit Systems: System Design and Effects'. In: p. 80. DOI: 10.3384/diss.diva-147049. URL: http://www.diva-portal.org/smash/get/diva2:1196452/FULLTEXT01.pdf.

Hatch, Jennie and John Helveston (2018). *Will Autonomous Vehicles be Electric?* URL: https://www.bu.edu/ise/2018/08/27/will-autonomous-vehicles-be-electric/.

Henning, K, H Preuschoff and J Happe (2003). 'Einsatzszenarien fur Fahrerassistenzsysteme im Gueterverkehr und deren Bewertung'. In: *FVDI Verlag GmbH* 525.

Hollander, Yaron and Ronghui Liu (2008). 'The principles of calibrating traffic microsimulation models'. In: *Transportation* 35.3, pp. 347–362. ISSN: 00494488. DOI: 10.1007/s11116-007-9156-2.

Jost, D. and K. Nagel (2005). 'Probabilistic traffic flow breakdown in stochastic car following models'. In: *Traffic and Granular Flow 2003*, pp. 87–103. DOI: 10.1007/3-540-28091-x{_}9.

Kanagaraj, Venkatesan et al. (2013). 'Evaluation of Different Vehicle Following Models Under Mixed Traffic Conditions'. In: *Procedia - Social and Behavioral Sciences* 104, pp. 390–401. ISSN: 18770428. DOI: 10.1016/j.sbspro.2013.11.132. URL: http://dx.doi.org/10.1016/j.sbspro.2013.11.132.

Kesting, Arne et al. (2008). 'Adaptive cruise control design for active congestion avoidance'. In: *Transportation Research Part C: Emerging Technologies* 16.6, pp. 668–683. ISSN: 0968090X. DOI: 10.1016/j.trc.2007.12.004.

Knoop, L. Victor (2017). *Macroscopic Traffic Flow Modelling Editor: Victor L. Knoop Reader from and for graduate Students Course by TRAIL research school*. Tech. rep. Delft: TU Delft, pp. 6–27. URL: https://www.victorknoop.eu/teaching/macroscopic_traffic_modelling.pdf.

KPMG (2019). '2019 Autonomous Vehicles Readiness Index: Assessing countries' preparedness for autonomous vehicles'. In: p. 60. URL: https://home.kpmg/br/pt/home/insights/2019/02/2019-autonomous-vehicles-readiness-index.html%0Ahttps://assets.kpmg/content/dam/kpmg/xx/pdf/2019/02/2019-autonomous-vehicles-readiness-index.pdf.

Krauß, Stefan (1998). 'Microscopic modeling of traffic flow: Investigation of collision free vehicle dynamics'. In: *D L R - Forschungsberichte* 8. ISSN: 14348454.

Kristoffersson, Ida and Anna Pernestål Brenden (2018). 'Scenarios for the development of self-driving vehicles in freight transport'. In: *7th Transport Research Arena TRA 2018*. URL: http://www.diva-portal.org/smash/get/diva2:1269611/FULLTEXT01.pdf.

Linköping University (2020). *Traffic Modeling and Simulation*. URL: https://liu.se/en/research/traffic-modelling-and-simulation.

Liu, Hao et al. (2018). 'Modeling impacts of Cooperative Adaptive Cruise Control on mixed traffic flow in multi-lane freeway facilities'. In: *Transportation Research Part C: Emerging Technologies* 95.December 2017, pp. 261–279. ISSN: 0968090X. DOI: 10.1016/j.trc.2018.07.027. URL: https://doi.org/10.1016/j.trc.2018.07.027.

Maurer, Markus et al. (2016). *Autonomous driving: Technical, legal and social aspects*, pp. 1–706. ISBN: 9783662488478. DOI: 10.1007/978-3-662-48847-8.

Milanés, Vicente and Steven E. Shladover (2014). 'Modeling cooperative and autonomous adaptive cruise control dynamic responses using experimental data'. In: *Transportation Research Part C: Emerging Technologies* 48, pp. 285–300. ISSN: 0968090X. DOI: 10.1016/j.trc.2014.09.001.

Moridpour, Sara, Geoff Rose and Majid Sarvi (2009). 'Modelling the heavy vehicle drivers' lane changing decision under heavy traffic conditions'. In: *32nd Australasian Transport Research Forum, ATRF 2009* December.

Müller, Stephan (2012). 'The Impact of Electronic Coupled Heavy Trucks on Traffic Flow'. In: *Gateways* 10, pp. 1–13.

Naus, G. J.L. et al. (2010). 'Design and implementation of parameterized adaptive cruise control: An explicit model predictive control approach'. In: *Control Engineering Practice* 18.8, pp. 882–892. ISSN: 09670661. DOI: 10.1016/j.conengprac.2010.03.012.

NTF (n.d.). *Högsta hastighet på motorväg?* URL: https://ntf.se/fragor-och-svar/trafikmiljo/hastighet/hogsta-hastighet-pa-motorvag/.

Olstam J., Tapani A. (2004). *Comparison of car-following models for simulation*. Tech. rep. Linköping: VTI. URL: https://www.vti.se/sv/publikationer/publikation/comparison-of-car-following-models_673977.

OpenStreetMap (2020). URL: https://www.openstreetmap.org/search?query=g%C3%B6teborg#map=14/57.7025/12.0025.

Pourabdollah, Mitra et al. (2018). 'Calibration and evaluation of car following models using real-world driving data'. In: *IEEE Conference on Intelligent Transportation Systems, Proceedings, ITSC* 2018-March.June 2018, pp. 1–6. DOI: 10.1109/ITSC.2017.8317836.

Ramezani, Hani et al. (2018). 'Micro-simulation of truck platooning with cooperative adaptive cruise control: Model development and a case study'. In: *Transportation Research Record* 2672.19, pp. 55–65. ISSN: 21694052. DOI: 10.1177/0361198118793257. URL: https://doi.org/10.1177/0361198118793257.

SAE (2019). *Levels of Driving Automation*. URL: https://www.sae.org/news/2019/01/sae-updates-j3016-automated-driving-graphic.

Sugimachi, Toshiyuki et al. (2013). *Development of autonomous platooning system for heavy-duty trucks ?* Vol. 7. PART 1. IFAC, pp. 52–57. ISBN: 9783902823434. DOI: 10.3182/20130904-4-JP-2042.00127. URL: http://dx.doi.org/10.3182/20130904-4-JP-2042.00127.

Tapani, Andreas (2008). *Traffic Simulation Modelling of Rural Roads and Driver Assistance Systems*. Norrköping, pp. 1–5. ISBN: 9789173938068. URL: https://www.diva-portal.org/smash/get/diva2:63/FULLTEXT01.pdf.

Tettamanti, Tamás, István Varga and Zsolt Szalay (2016). 'Impacts of autonomous cars from a traffic engineering perspective'. In: *Periodica Polytechnica Transportation Engineering* 44.4, pp. 244–250. ISSN: 15873811. DOI: 10.3311/PPtr.9464.

Trafikverket (2013). *Handbok för kapacitetsanalys*. URL: https://www.trafikverket.se/contentassets/32ce05ecc3ac458bb8ecb802e8e2da54/handbok_for_kapacitetsanalys_med_hjalp_av_simulering.pdf.

– (2014). *Kapitel 6 Trafikprognoser och prognosmodeller*. Tech. rep. Borlänge: Trafikverket.

– (2019). *Detector data*. Borlänge.

TRB (2000). *Highway capacity manual*, pp. 1–1207. ISBN: 0-309-06681-6.

Treiber, Martin and Arne Kesting (2013). *Traffic Flow Dynamics*. ISBN: 9783642324598. DOI: 10.1007/978-3-642-32460-4.

Ye, Fan and Yunlong Zhang (2009). 'Vehicle type-specific headway analysis using freeway traffic data'. In: *Transportation Research Record* 2124, pp. 222–230. ISSN: 03611981. DOI: 10.3141/2124-22.

Yuan, K, Victor L. Knoop and Serge P. Hoogendoorn (2014). 'Capacity Drop : a Relation Between the Speed In Congestion And The Queue Dicharge Rate'. In: *Transportation Research Record: Journal of the Transportation Research Board* 2491, pp. 72–80.

Zaidi, Kamran et al. (Jan. 2015). 'Data-centric rogue node detection in VANETs'. In: *Proceedings - 2014 IEEE 13th International Conference on Trust, Security and Privacy in Computing and Communications, TrustCom 2014*. Institute of Electrical and Electronics Engineers Inc., pp. 398–405. ISBN: 9781479965137. DOI: 10.1109/TrustCom.2014.51.